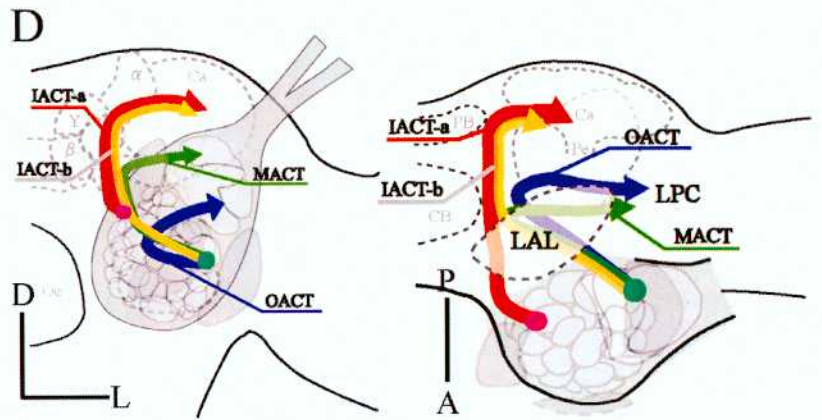
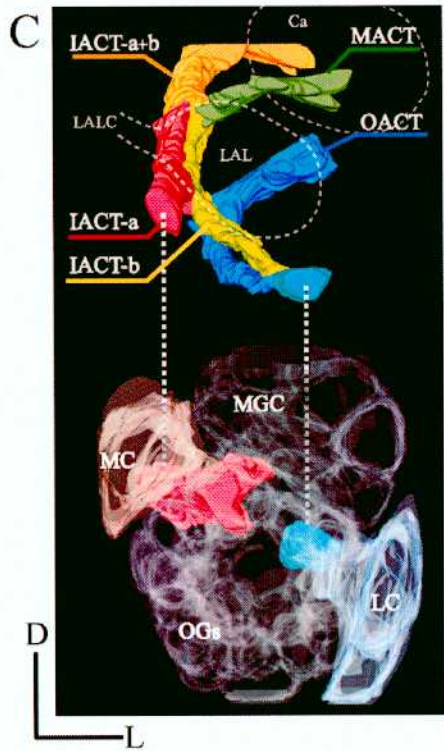
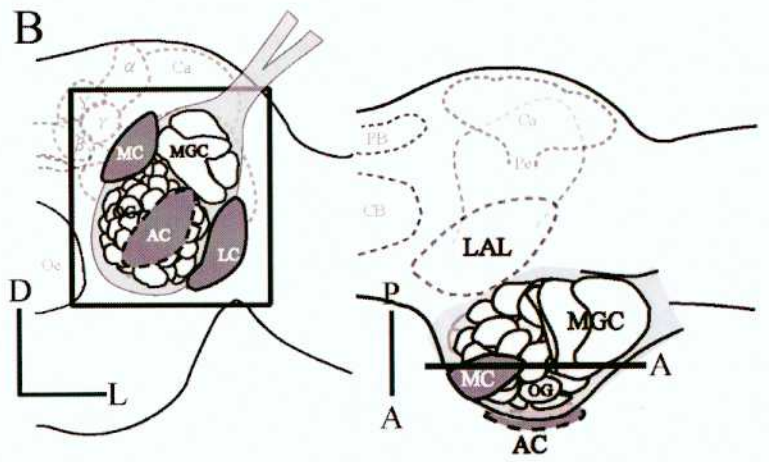
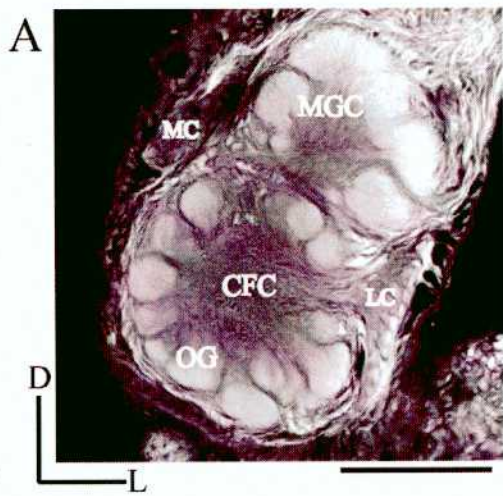
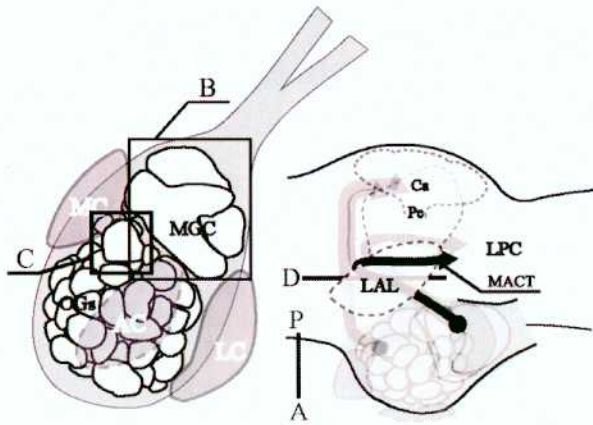
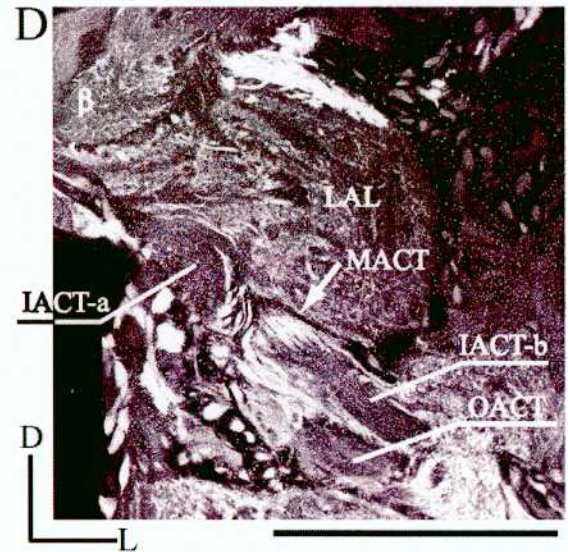
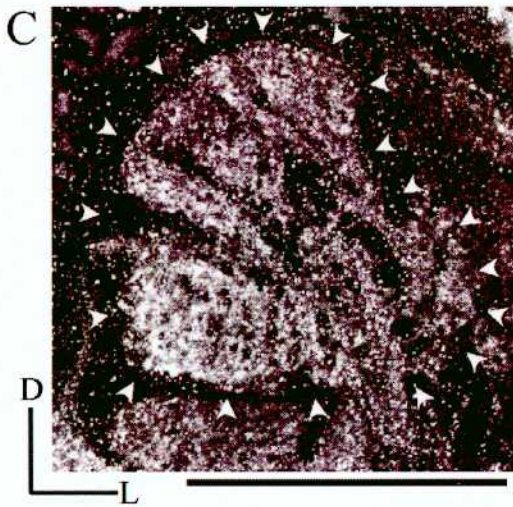
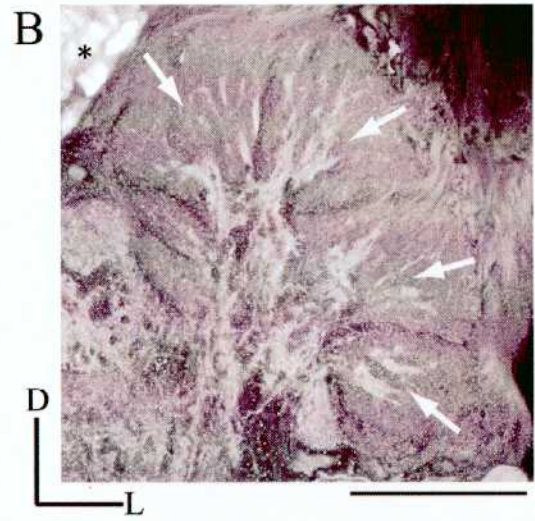
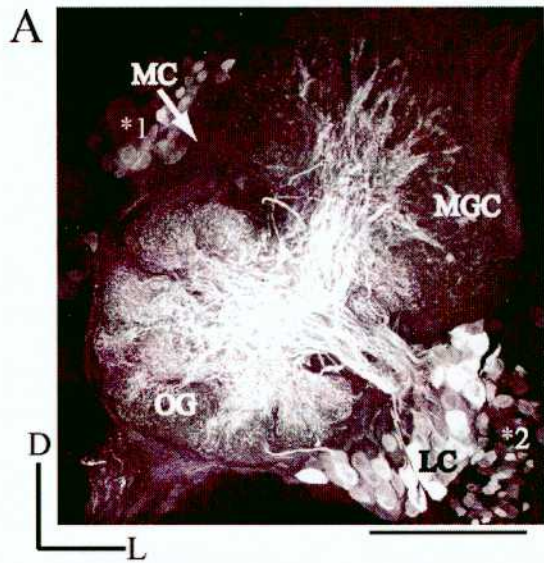


## **Figures and legends**

**Fig. 1.** Position and internal organization of the antennal lobe (AL). A) Confocal slice image of the Lucifer Yellow stained two cell clusters and the neural structures in the AL. The cell clusters were the medial cell cluster (MC) and the lateral cell cluster (LC). The AL neural structure consisted of a center fiber core (CFC), ordinary glomeruli (OG) and the macroglomerular complex (MGC). Scale bar: 100  $\mu$ m, D: dorsal, L: lateral, B) Frontal (left) and dorsal (right) diagram of the cell cluster and the neural structures of the AL. The anterior cell cluster (AC) was added on diagram. The areas in the box and horizontal line are depicted in (A). P: posterior, A: anterior, C) Reconstruction of the antenno-cerebral tracts (ACT) and surrounding neural structures. The dashed line links processes that were separated to reveal the neural structures that overlapped *in situ*. The AL was connected to the protocerebrum (PC) by the inner, middle and outer antenno-cerebral tracts (IACT, MACT and OACT). IACT was classified into IACT-a and IACT-b due to the originating positions. The ACT distribution surrounded the lateral accessory lobe (LAL) and innervated the protocerebrum (PC) D) Frontal (left) and dorsal (right) diagram of the ACT to the PC.



**Fig. 2.** GABA immunolabeling in the AL. A) Confocal projection image of the AL (thickness: 98.0  $\mu\text{m}$ ). GABA immunopositive cell bodies were observed in the lateral cell cluster (LC) but not in the MC (arrow). Immunoreactive fibers arborized in the CFC, all OGs and each compartment of the MGC. Asterisk 1 shows a cell cluster of the protocerebrum (PC). Asterisk 2 shows a cell cluster in the optic lobe. B) Confocal slice image of the MGC. Immunoreactive branchings were restricted to some small partitions in the MGC compartments (arrows). The asterisk shows a cell cluster of the PC. C) Confocal slice image of the OGs. Immunoreactive arborization was distributed in the whole region of each OG (surrounded by the arrowheads). D) Confocal slice image of the protocerebrum. Some immunoreactive axons ran through the MACT (arrow). Inset: schematic diagrams of the frontal AL (left) and the dorsal hemisphere of the brain (right). The area in the box and horizontal lines are depicted in (B-D). Scale bars: 100  $\mu\text{m}$



**Fig. 3.** FMRFamide immunolabeling in the AL. A) Confocal projection image of the AL (thickness: 121.6  $\mu\text{m}$ ). FMRFamide immunopositive cell bodies were observed in the lateral cell cluster (LC). Immunoreactive fibers arborized in the CFC and in all the OGs and the MGC. B) Confocal slice image of the medial cell cluster (MC). Immuno positive cell bodies were not located in the MC. C) Confocal slice image of the anterior cell cluster (AC) and LC. Immunopositive cell bodies were observed in the AC and LC. D) Confocal slice image of the OGs and MGC. Immunoreactive arborization was distributed in the whole region of each OG (surrounded by the arrowheads) and MGC. E) Confocal slice image of the protocerebrum region. A few immunoreactive axons ran through the OACT (arrow) F) Confocal slice image of the protocerebrum region. A few immunoreactive axons ran through the MACT (arrow). Inset: schematic diagrams of the frontal AL (left) and the dorsal hemisphere of the brain (right). The areas in the box and horizontal lines are depicted in (B-F). Scale bars: 100  $\mu\text{m}$

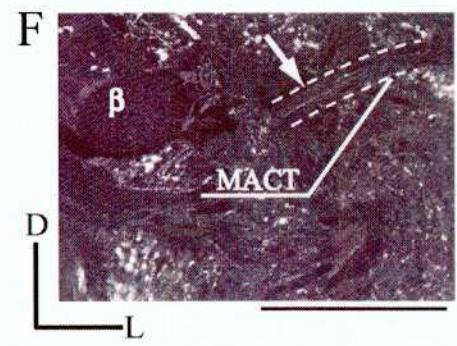
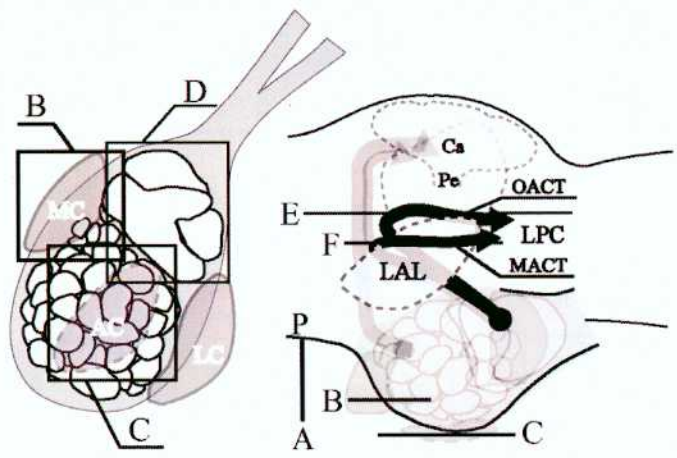
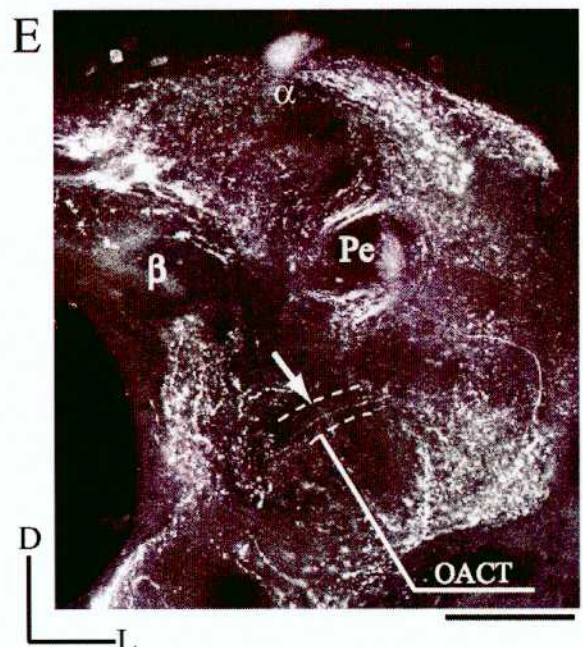
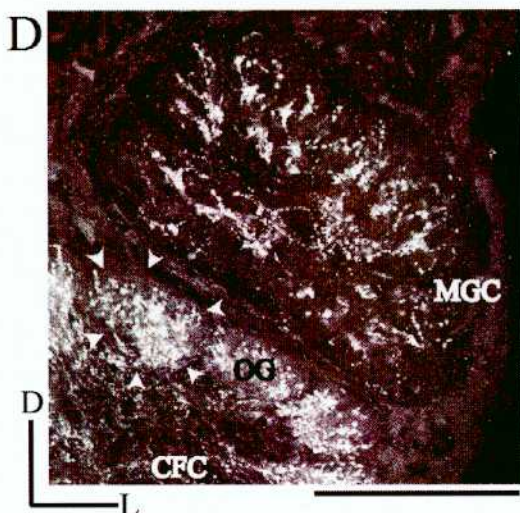
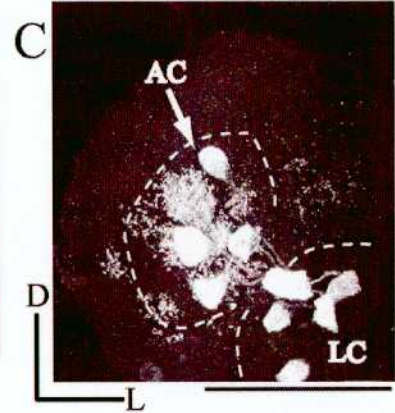
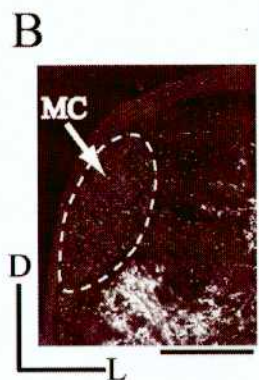
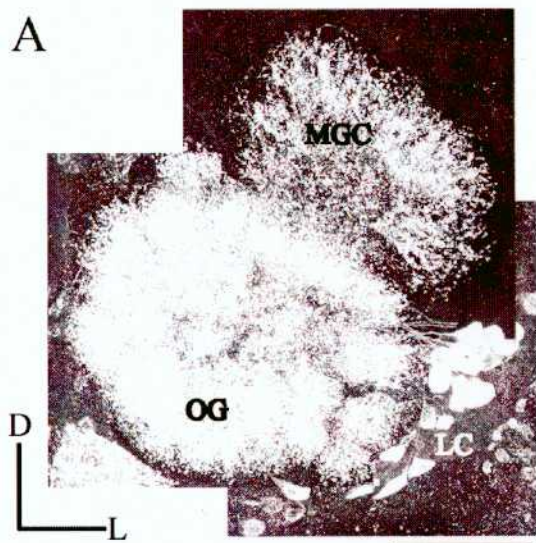


**Fig. 4.** Serotonin immunolabeling in the AL. A) Confocal projection image of the AL (thickness: 122.4  $\mu\text{m}$ ). Immunoreactive fibers arborized in the CFC, OGs and each compartment of the MGC. B) Confocal projection image of the posterior region of the AL (10.4  $\mu\text{m}$ ). A single serotonin immunoreactive cell body was observed in the boundary region between the lateral cell cluster (LC) and the protocerebrum (PC). C) Confocal slice image of the OGs and MGC. In the OGs, immunoreactive arborization was restricted to the interior side (arrow 1). In the MGC, immunoreactive branchings were restricted to some small partitions (arrow 2). D) Confocal slice image of the protocerebrum. Two immunoreactive axons ran through the IACT-b (arrow). Inset: schematic diagrams of the frontal AL (left) and the dorsal hemisphere of the brain (right). The areas in the box and horizontal lines are depicted in (B-D). Scale bars: 100  $\mu\text{m}$



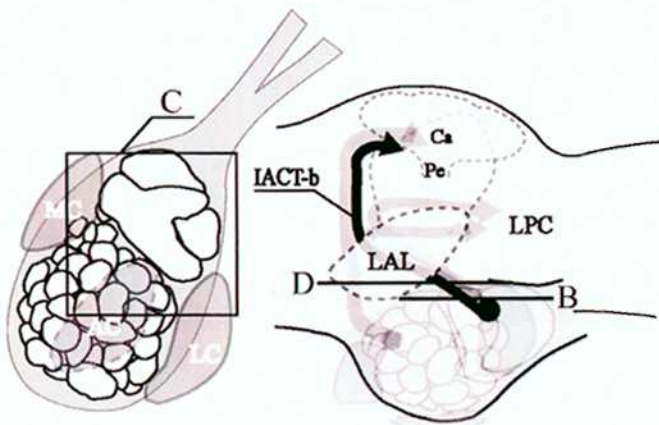
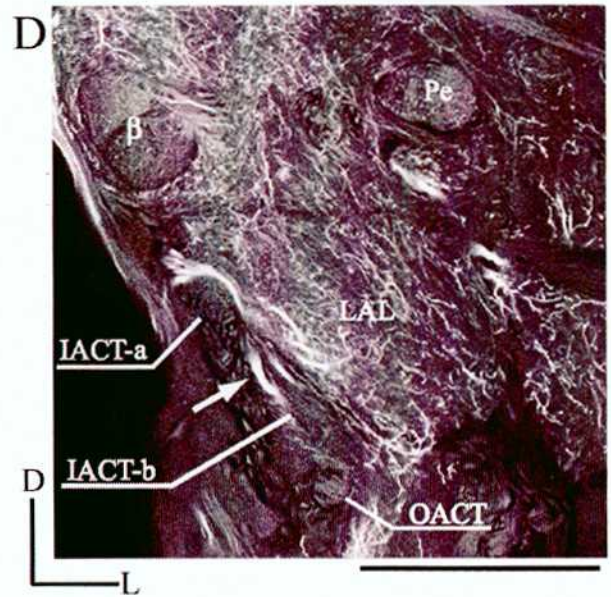
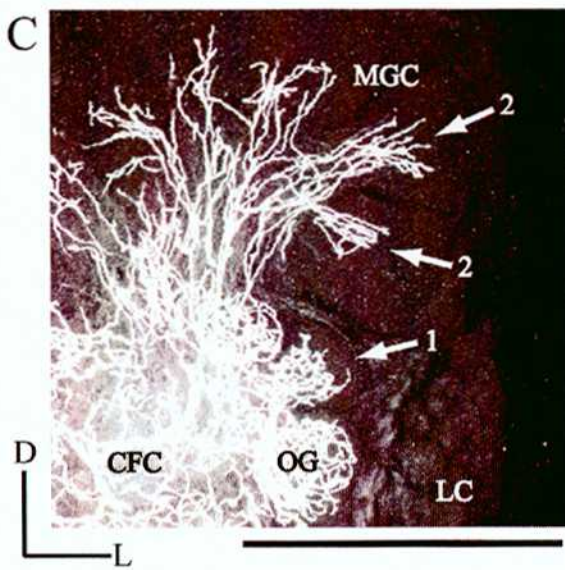
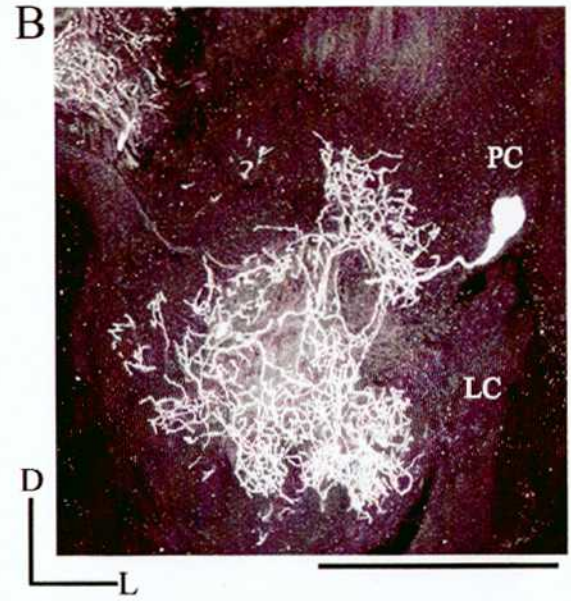
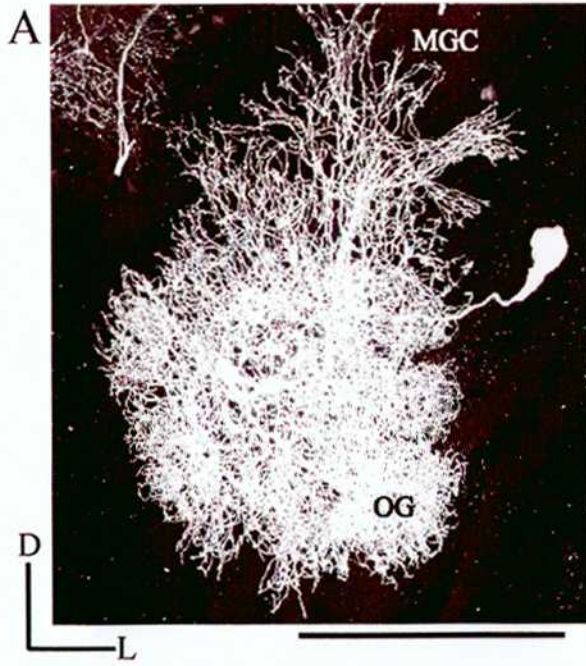


**Fig. 5.** Serotonin immunocytochemical double labeling for the candidate AL neuron elected from Neuron Database. A) Lucifer yellow stained fiber in the AL. B) Serotonin immunoreactive fibers in the AL. C) Both superimposed. Yellow color showed overlap between green color and red color. This yellow color proved serotonin immunocytochemical double labeling had succeeded. Inset: schematic diagrams of the frontal AL. The area in the box is depicted in (A-C). Scale bars: 100  $\mu\text{m}$

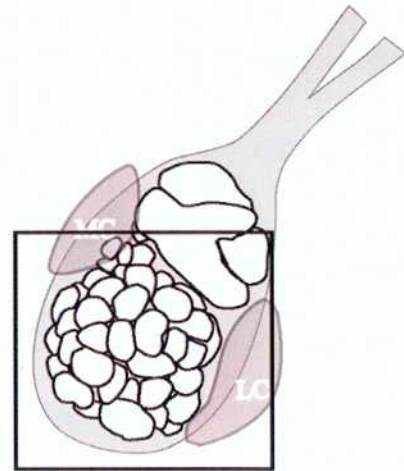
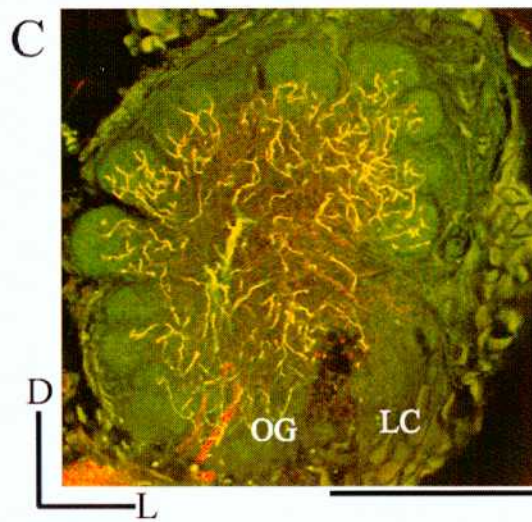
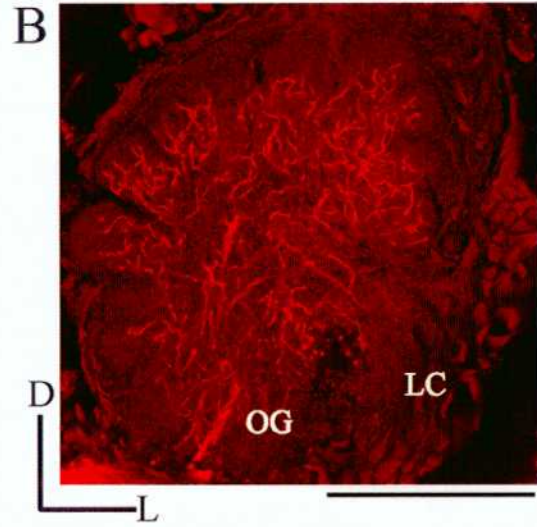
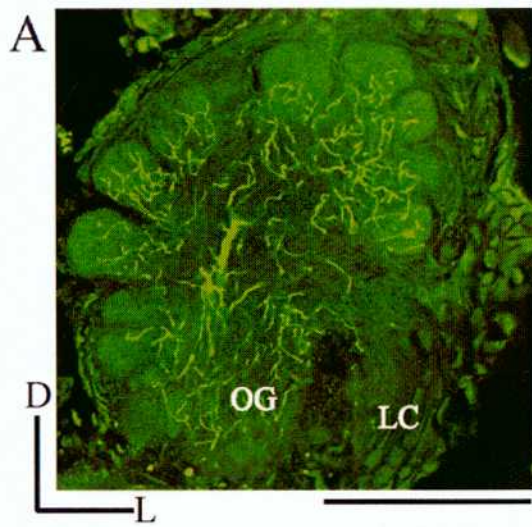
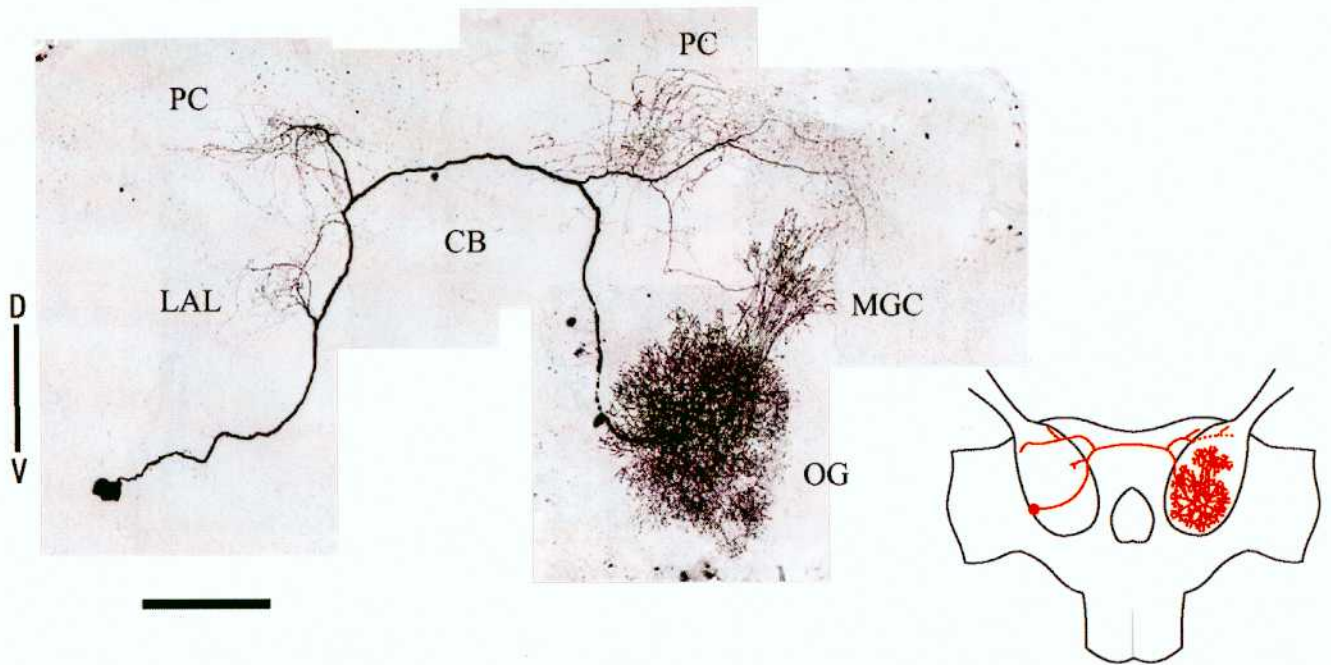


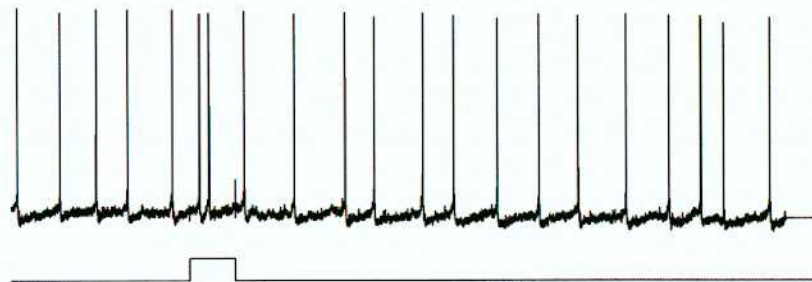
**Fig. 6.** Morphology and physiology of serotonin immunoreactive AL neuron identified by serotonin immunocytochemical double labeling (Fig. 5). A) The cell body was located in the boundary region between the lateral cell cluster and the protocerebrum and branched throughout the contralateral AL. This neuron also had processes in both the ipsilateral and contralateral superior protocerebrum, the ipsilateral LAL, the calyces of both mushroom bodies, and in the central body. Examination of individual optical sections revealed that this neuron branched in every OGs, and each compartment of the MGC. The primary neurite of this neuron projected through the ipsilateral AL where it had a few fine branches in the posterior coarse neuropil region of the AL. Morphology of serotonin immunoreactive AL neuron elected from the Neuron Database. This neuron was stained by Dr. Evan S Hill. B) This neuron fired spontaneously with long action potentials, and showed a delay response to all stimulation to the antennae. This physiological property indicated that this neuron responds to mechanosensory stimulation. Physiology of serotonin immunoreactive AL neuron elected from the Neuron Database. This physiology was recorded by Ms. L. Gatellier. Scale bars: 100  $\mu\text{m}$

A

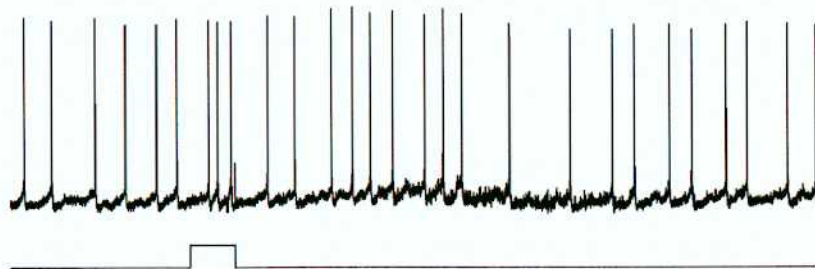


B

Bombykol



Bombykal



Control

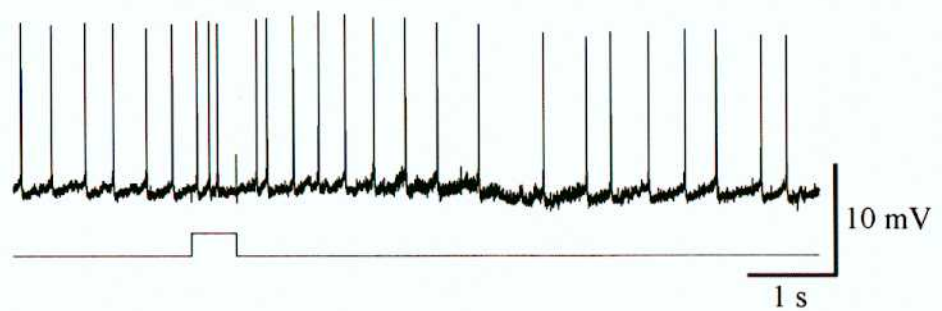
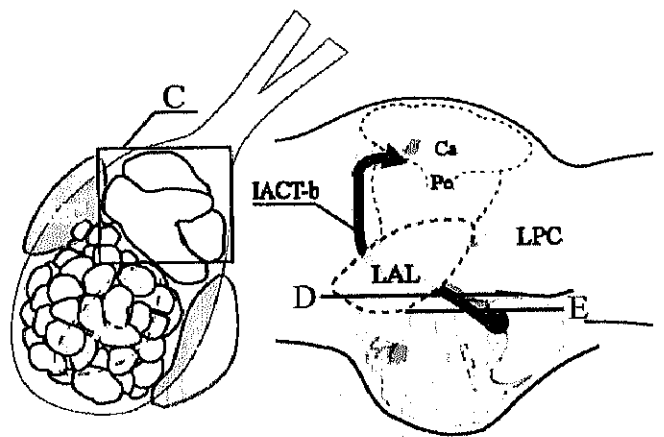
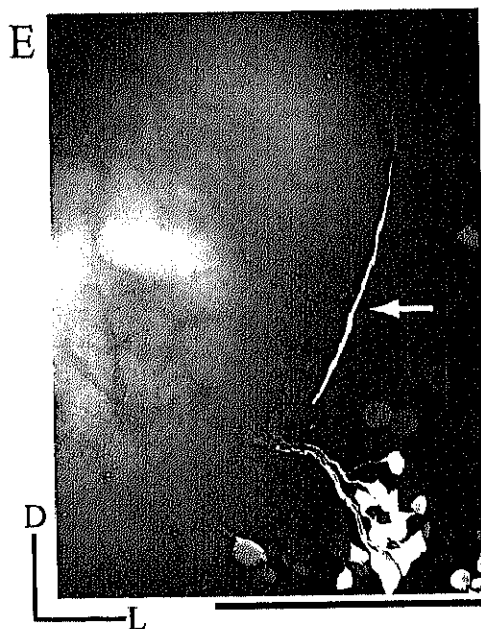
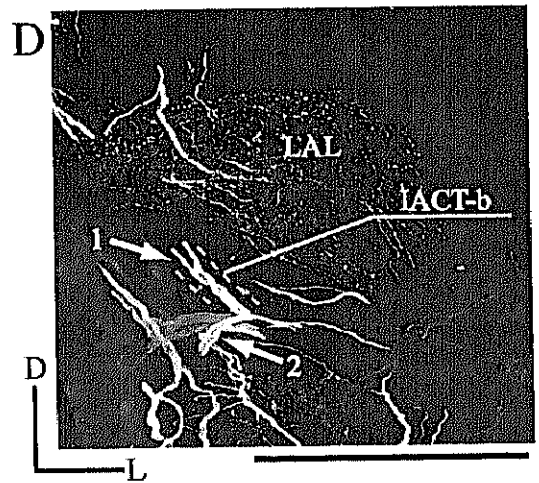
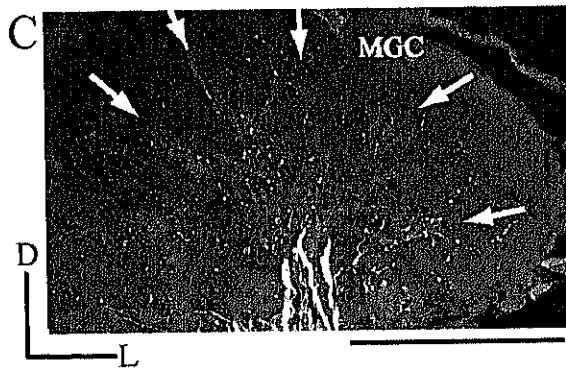
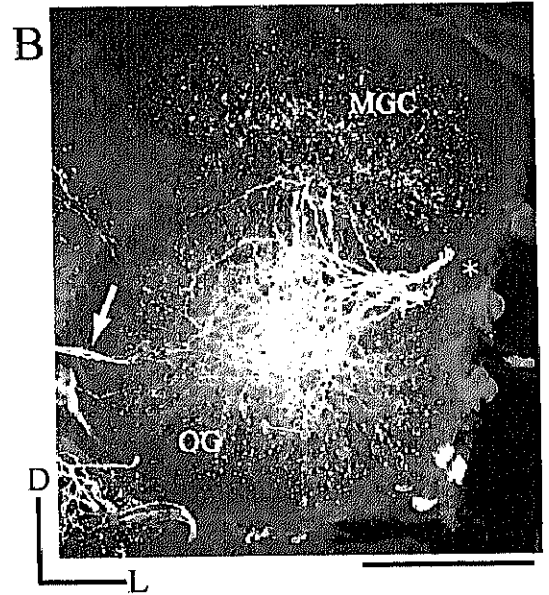
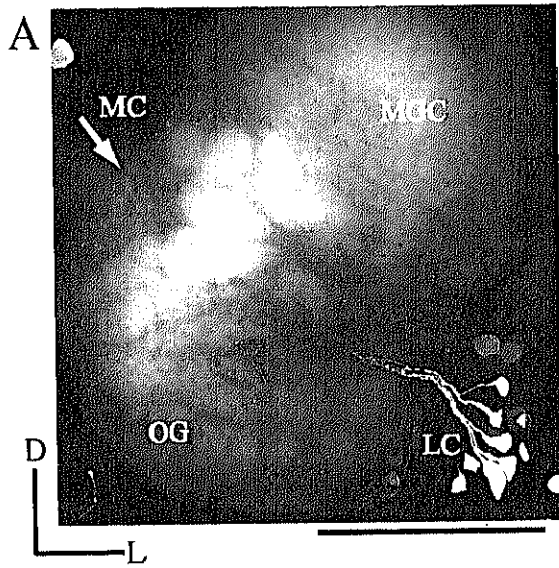
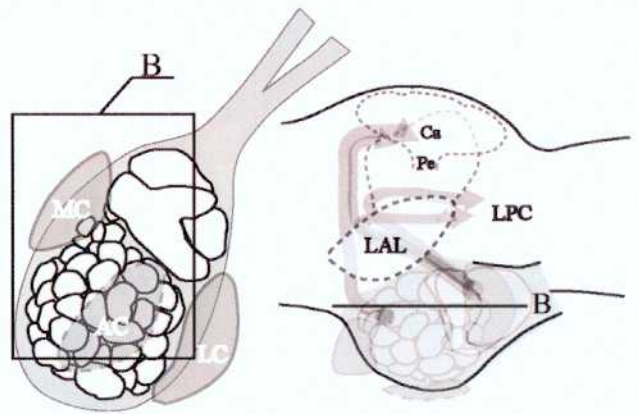
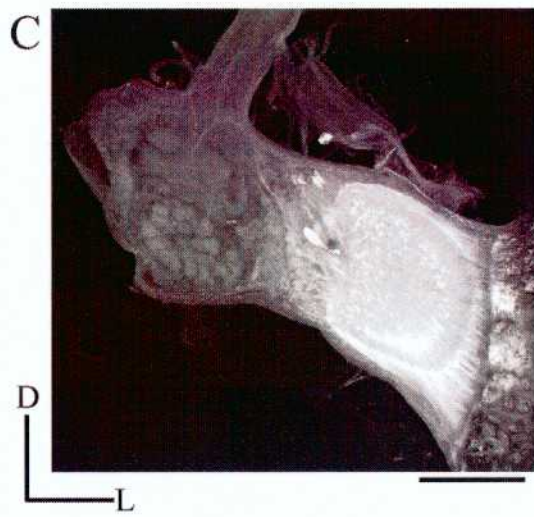
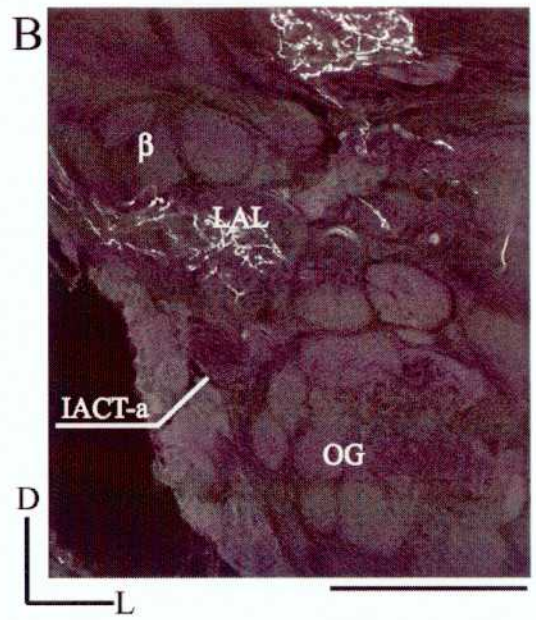
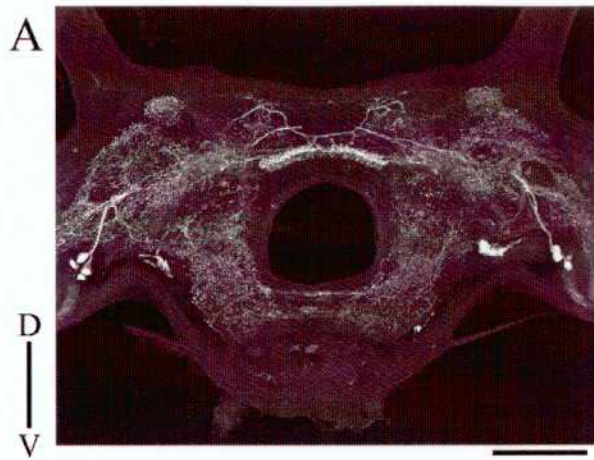


Fig. 7. Tyramine immunolabeling in the AL A) Confocal projection image of the AL (thickness: 76.8  $\mu\text{m}$ ). Tyramine immunopositive cell bodies were observed in the lateral cell cluster (LC) and their primary neurites, but not in the medial cell cluster (MC) (arrow). Immunoreactive fibers arborized in the CFC, OG and each compartment of the MGC. Immunoreactive patterns usually were restricted to the medial side of the OGs. B) Confocal projection image of the AL (thickness: 180.8  $\mu\text{m}$ ). Immunoreactive intensity fluctuated with the preparation. Immunoreactive arborizations in the AL usually linked to two immunoreactive axons in the IACT-b (arrow). Asterisk shows the inadvertent cracking of the LC. C) Confocal slice image of the MGC. Immunoreactive branchings were restricted to some small partitions in the MGC compartments (arrows). D) Confocal projection image of the protocerebrum region (thickness: 25.6  $\mu\text{m}$ ). Two immunoreactive axons were observed in IACT-b (arrow 1). Two immunoreactive neurites also innervated toward the suboesophageal ganglion (SOG) (arrow 2). E) Confocal projection image of the posterior region of the AL (thickness: 32.8  $\mu\text{m}$ ). In the lateral side of the antennal nerve (AN), immunoreactive axons were observed (arrow). Inset: schematic diagrams of the frontal AL (left) and the dorsal hemisphere of the brain (right). The areas in the box and horizontal lines are depicted in (C-E). Scale bars: 100  $\mu\text{m}$



**Fig. 8.** Histamine immunolabeling in the brain of the silkworm moth. A) Confocal projection image (thickness: 198.8  $\mu\text{m}$ ), histamine immunoreactivity was observed in the protocerebrum (PC). Scale bar: 200  $\mu\text{m}$  B) Confocal slice image of the AL. Histamine immunoreactivity was not observed in the cell clusters, glomerular structures and the projection pathways of the AL. Scale bar: 100  $\mu\text{m}$  C) Confocal projection image (thickness: 193.2  $\mu\text{m}$ ), histamine immunoreactivity was observed in the optic lobe, but not in the AL and in AN. Scale bar: 200  $\mu\text{m}$ . Inset: schematic diagrams of the frontal AL (left) and the dorsal hemisphere of the brain (right). The areas in the box and horizontal lines are depicted in (B).





**Fig. 9.** Position and internal organization of the lateral accessory lobe (LAL) and ventro lateral protocerebrum (VPC) regions as revealed by serotonin-immunostaining. A) Schematic diagram of the frontal moth brain. The boxed area shows the region depicted in (D-F). B) Schematic diagram of the moth brain. Horizontal line of the right side LAL and VPC region reveals the depth in (D-F). C) 3-D reconstruct diagram of the relationship between major antenno-cerebral tract (OACT) location and one side of the LAL-VPC neural structure. D-F) Frontal sections through the LAL and VPC regions at anterior D), middle E), and posterior F) depth from its anterior surface. Depth diagram shows in B). D) Confocal slice image of the LAL and VPC regions on the anterior depth. LAL and VPC neuropil structures divided and surrounded by LALC (orange dotted arrow head), IACT-a (skyblue dotted arrow head), IACT-b (skyblue dotted arrow head), OACT (deepblue dotted arrow head), and descending pathway of GII descending neurons (yellow dotted arrow head). E) Confocal slice image of the LAL and VPC regions on the middle depth. LALC divides LAL neural structure into ventro-medial LAL (vmLAL) subregion and dorso-lateral LAL (dlLAL) subregion. F) Confocal slice image of the VPC regions on the posterior depth. LAL and VPC are divided by OACT (deepblue dotted arrow head). LALC divides VPC neural structure into medial VPC (mVPC) subregion and lateral VPC (lVPC) subregion. G) Single cell staining with intracellular recording also reveal LALC divided the VPC into mVPC and lVPC. Scale bars: 100  $\mu$ m in D-G.

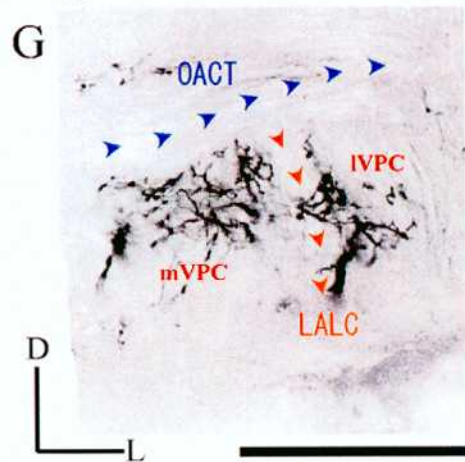
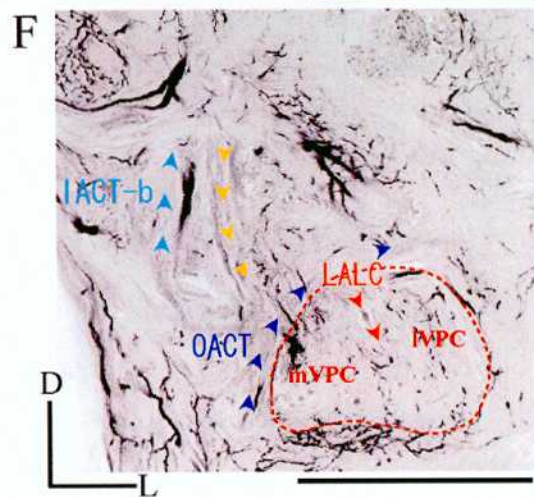
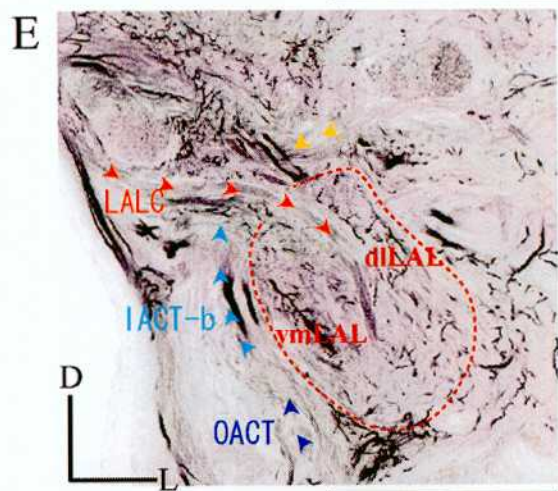
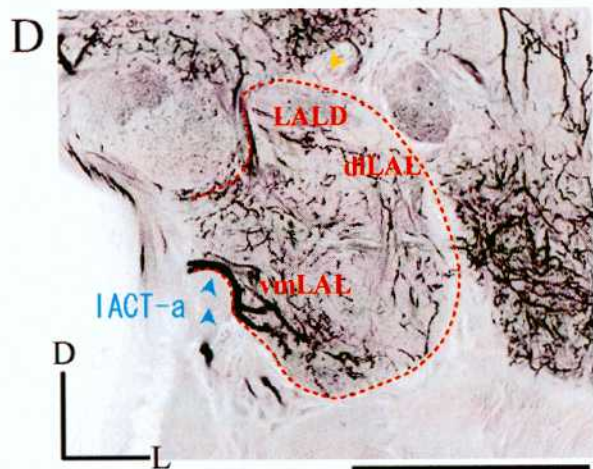
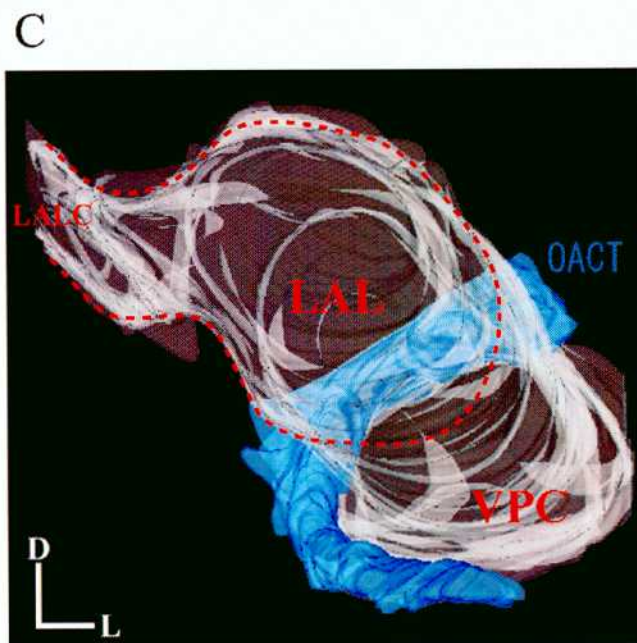
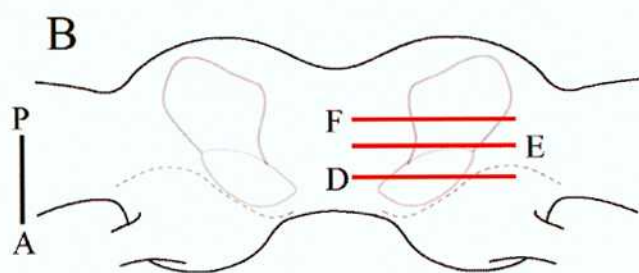
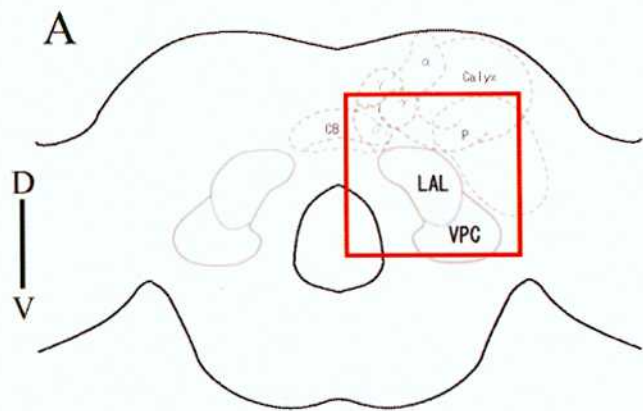


**Fig. 10.** Typical morphology of Type-A LAL-BLs elected from the Neuron Database. This neuron was stained by Dr. Tsuneko Kumagai A) This neuron restricted its branches entirely to both sides of the LAL. The cell body was located just posterior at the dorsal side of medial cell cluster in the AL and side of the  $\gamma$ -lobe of the mushroom body. The primary neurite ran ventrally to the ipsilateral LAL, where restrictly distributed in vmLAL and IVPC subregion, smooth branches were observed. The main neurite crossed the brain via the LAL commissure and arborized in vmLAL of contralateral profusely. These arbors exhibited remarkable varicose characteristics. B) Dorsal view. C) Location diagram of A. D) Location diagram of B. Refer from the Neuron Database, this neuron responded with long-lasting excitation to antennal stimulation with bombykol. Scale bars: 100  $\mu\text{m}$  in A-B

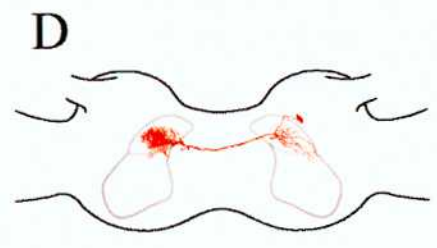
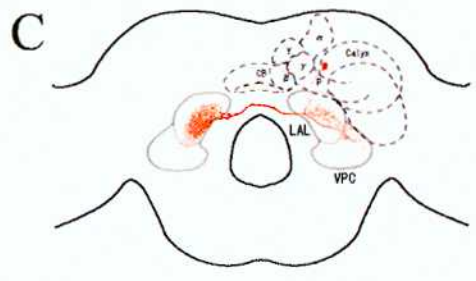
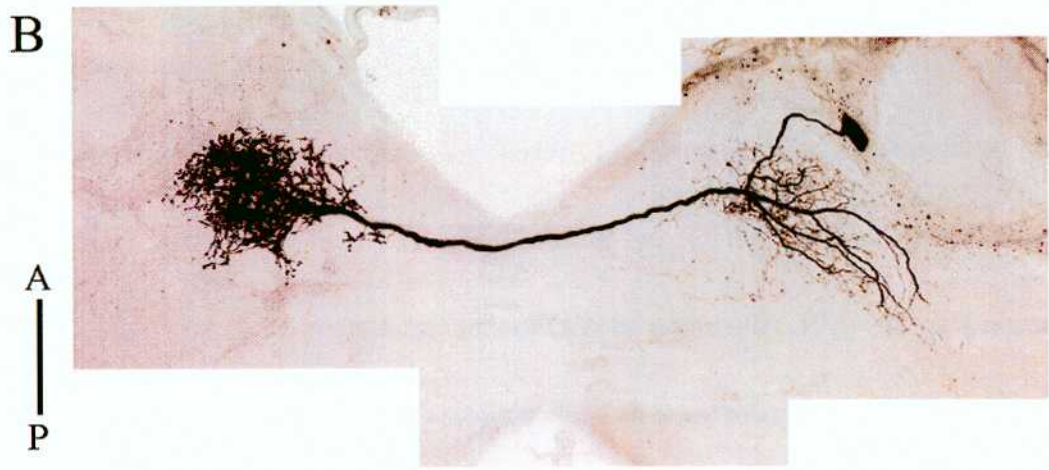
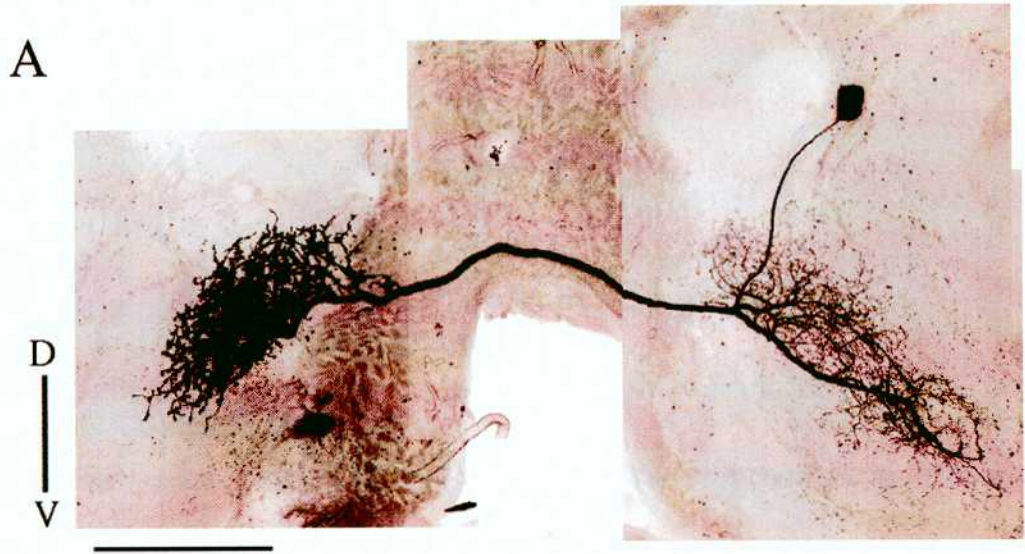


**Fig. 11.** Typical morphology of Type-B LAL-BLs elected from the Neuron Database. This neuron was stained by Dr. Tatsuya Mishima A) The cell body was located on dorsal and posterior position in the brain just ventrally to the edge of the calyx, where lateral side in the middle line of the mushroom body calyx. The main neurite ran forwardly to ipsilateral LAL, where it formed biasedly smooth branched in dLAL and IVPC subregion restrictly distribution pattern. The main neurite crossed the midline of the brain via the LAL commissure through the contralateral LAL, where it formed widely varicose terminals that were distributed in vmLAL, dLAL and IVPC. B) Dorsal view. C) Location diagram of A. D) Location diagram of B. According to the Neuron Database, this neuron responded with long-lasting inhibition to antennal stimulation with bombykol. Scale bars: 100  $\mu\text{m}$  in A-B

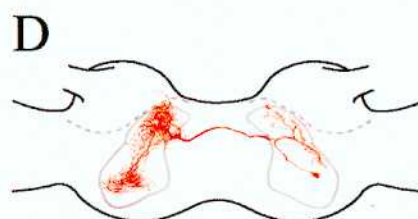
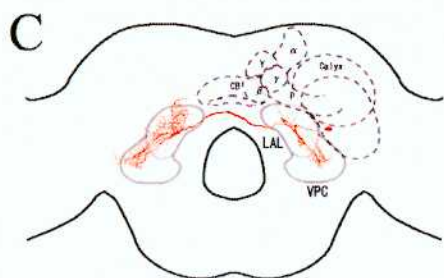
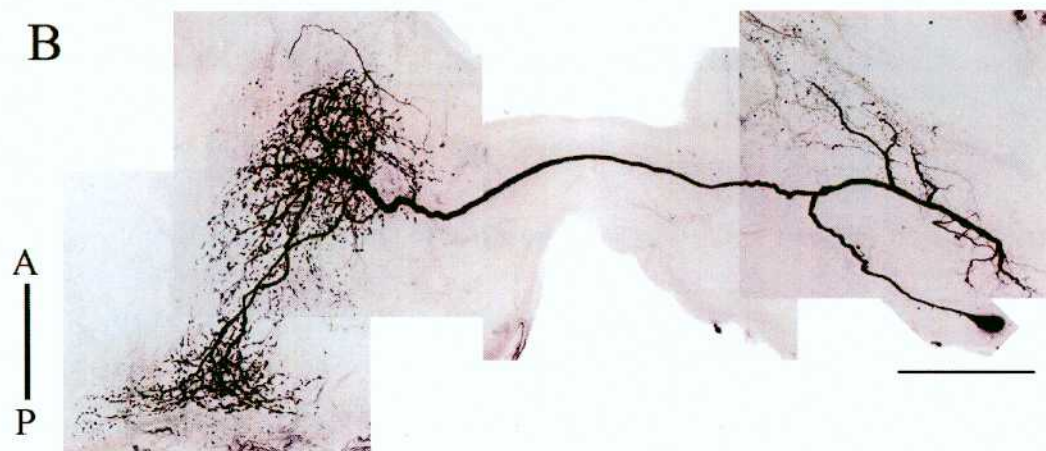
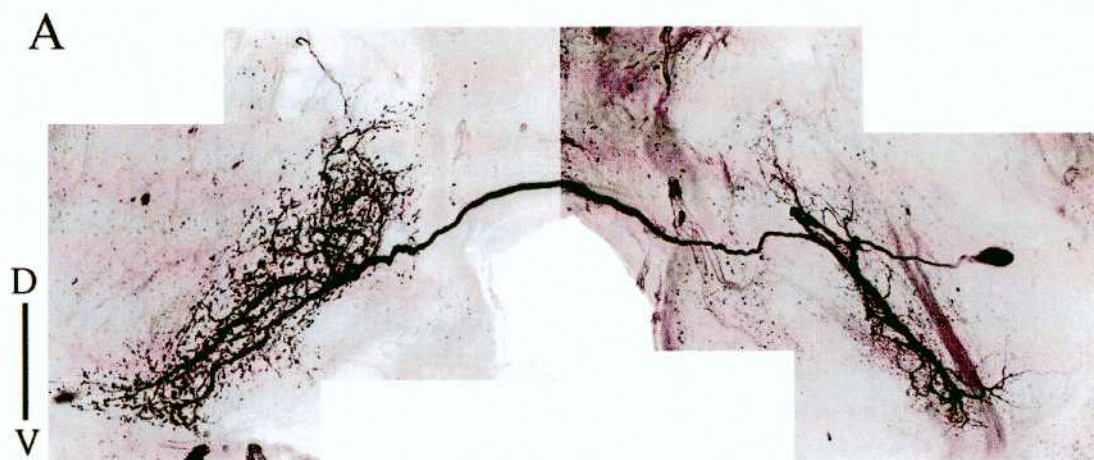


**Fig. 12.** Typical morphology of Type-A LAL-VPC LNs elected from the Neuron Database. This neuron was stained by Mr Akio Mori A) This neuron was located in just anterior of the neurite route of IACT-a, IACT-b and other tract, where passage of ventro-medial side in LAL. The primary neurite, which left from somata, ran ventro-laterally and trace outline of OACT ventro-laterally, where the neurite divided in two axons. One neurite projected anteriorly and then made smooth arbors in the whole area of LAL (vmLAL and dlLAL). A second neurite projected posteriorly and then several conspicuous varicose terminals extending into the wide spread of VPC (mVPC and lVPC). B) Dorsal view. C) Anterior projection view of LAL region, referenced by OACT location. Only smooth arborization were confirmed. D) Posterior projection view of VPC region, referenced by OACT location. Only varicose processes were confirmed. E) Location diagram of A. F) Location diagram of B. According to the Neuron Database, this neuron responded with recurrent brief excitation to antennal stimulation with full pheromone component (mixture of bombykol and bombykal). Scale bars: 100 $\mu$ m in A-D



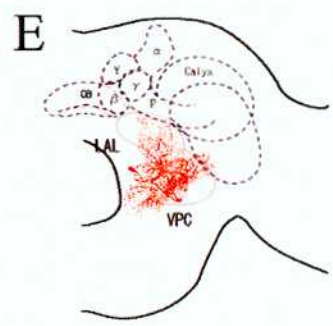
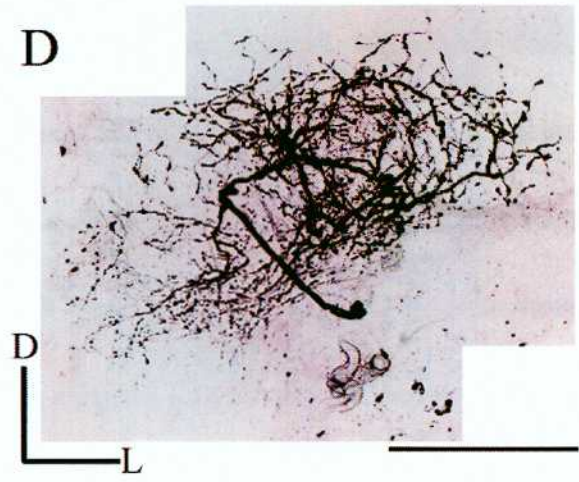
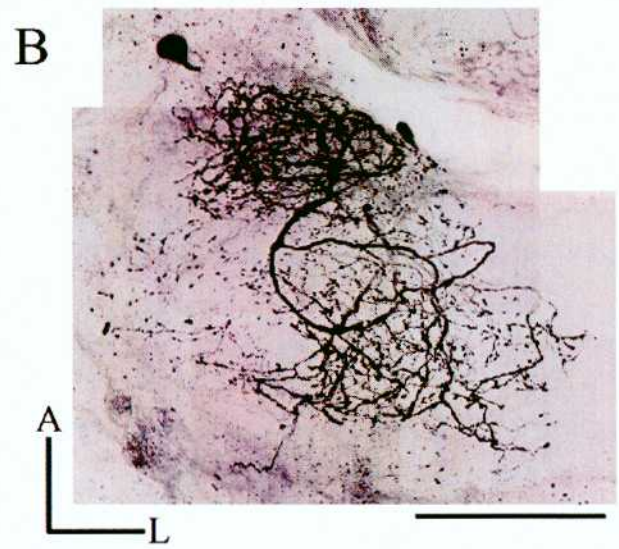
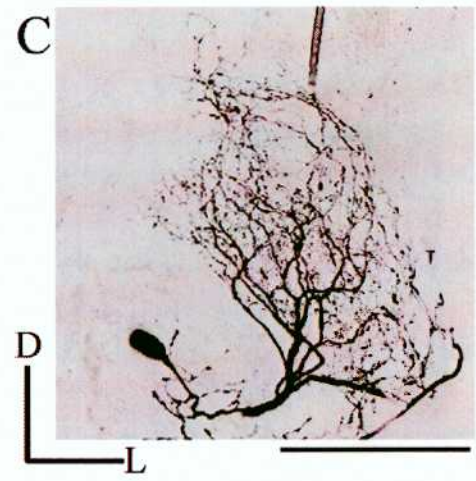
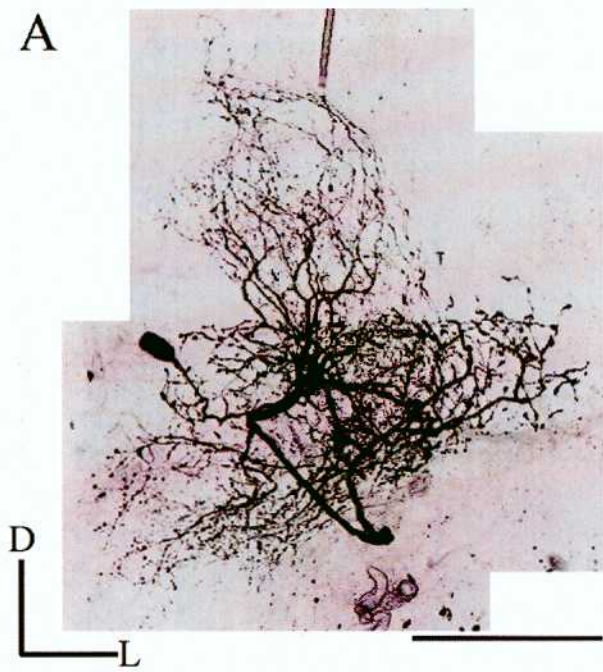


**Fig. 13.** Typical morphology of Type-B- $\alpha$  LAL-VPC LNs elected from the Neuron Database. This neuron was stained and recorded by Mr Akio Mori A) The cell body was located on dorsal side of protocerebrum bridge. The primary neurite ran ahead to the anterior divided region of LAL and VPC medially, where it innervated to LAL-VPC region from the adjacent winding point of OACT. On this position, the stout axon parted smooth branches on the whole VPC region (mVPC and IVPC) mainly and varicose terminals on the whole LAL region (vmLAL and dlLAL) mainly. From detail observation, the axon, which made varicose terminals on LAL, had second neurite on the border region of LAL and VPC, defined mVPC anterior region (mVPCa). Even on this part, I could identify petty varicose terminals. B) Dorsal view. Secondary varicose processes were observed in the mVPC anterior region (black arrow) C) Anterior projection view of the LAL, referenced by OACT location. Only varicose processes were confirmed. D) Posterior projection view of VPC region, referenced by OACT location. Only smooth arborization were confirmed. E) Location diagram of A. F) Location diagram of B. According to the Neuron Database, this neuron responded with later brief excitation to antennal stimulation with bombykol. Scale bars: 100 $\mu$ m in A-D

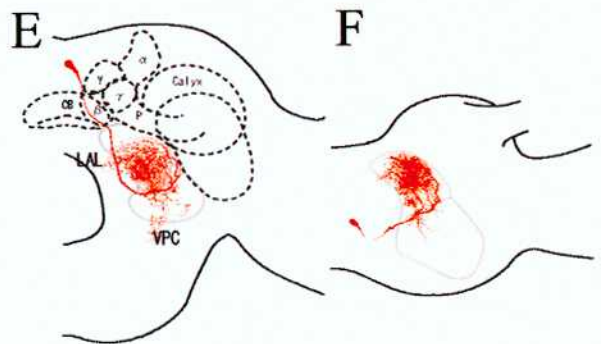
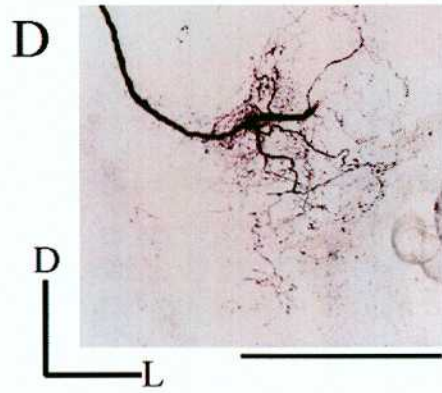
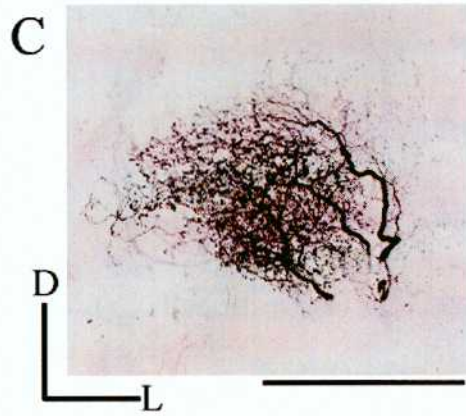
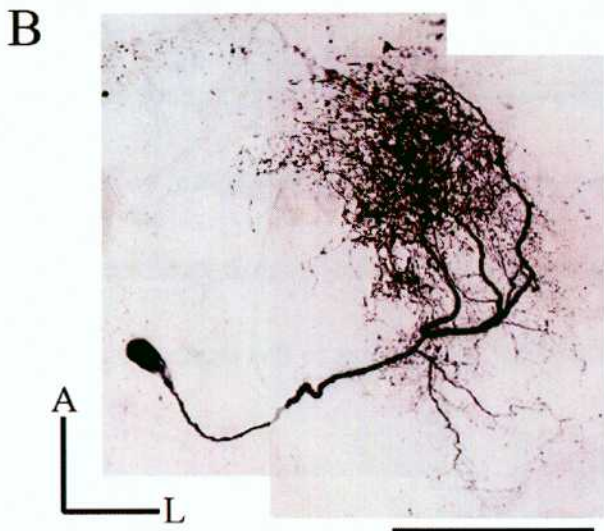
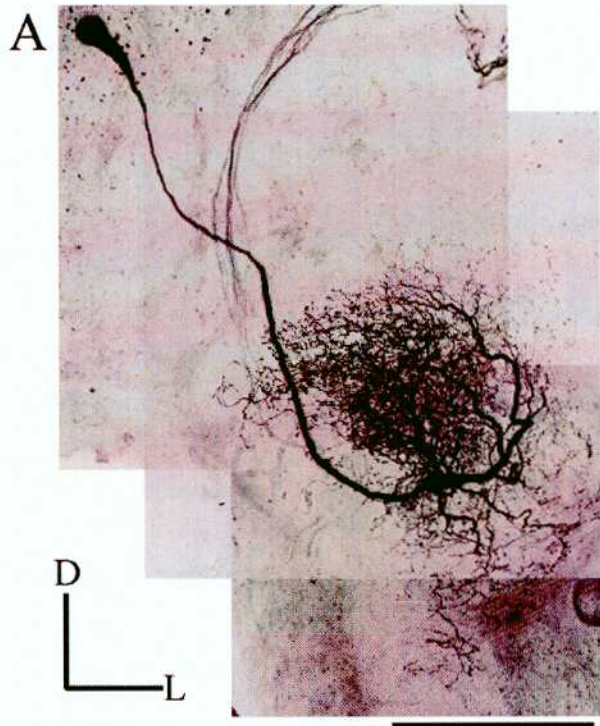


**Fig. 14.** Typical morphology of Type-B- $\beta$  LAL-VPC LNs elected from the Neuron Database. This neuron was stained and recorded by Dr. Tatsuya Mishima A) The cell body of this neuron was located in just anterior of the neurite route of IACT-a, IACT-b and other tract, where passage of ventro-medial side in LAL. The primary neurite, which left from the somata, ran ventro-laterally and trace outline of OACT ventro-laterally, where the neurite arrived on border region of LAL and VPC. Where the main neurite made conspicuously smooth branches in mVPCa (black arrow), and this neuron ascended its neurite toward the vmLAL. On vmLAL, this neuron formed distinct varicose terminals. B) Dorsal view. Varicose processes were observed in mVPC anterior region where divided by OACT. C) Anterior projection view of LAL region, referenced by OACT location. Only varicose processes were confirmed. D) Posterior projection view of VPC region, referenced by OACT location. Only smooth arborization was confirmed. E) Location diagram of A. F) Location diagram of B. According to the Neuron Database, this neuron exhibited a characteristic long-lasting excitation caused by bombykol stimulation to the antenna. Scale bars: 100 $\mu$ m in A-D

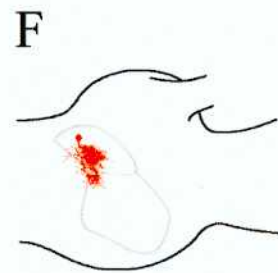
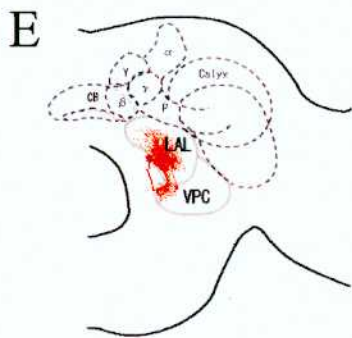
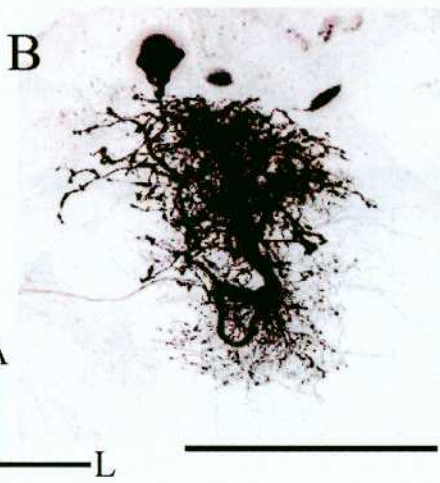
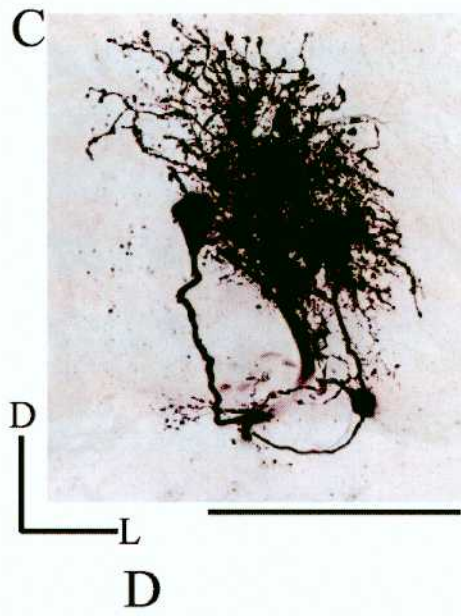
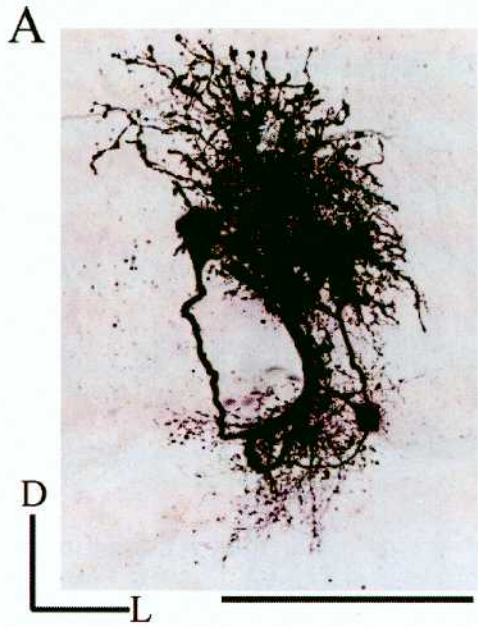


**Fig. 15.** Distribution pattern of GABA immunoreactivity in the LAL region A) Confocal slice image of the LAL region. Immunoreactive fibers were observed in the whole LAL region. Some immunoreactive axons ran through the frontal area of the LALC and connected to each side of the LAL regions bilaterally (arrow). B) GABA immunoreactive cell cluster was observed in the lateral side of the  $\gamma$ -lobe of the mushroom body (arrow1). Some GABA immunoreactive neurites ran through to the LAL region from immunoreactive cell cluster (arrow2).

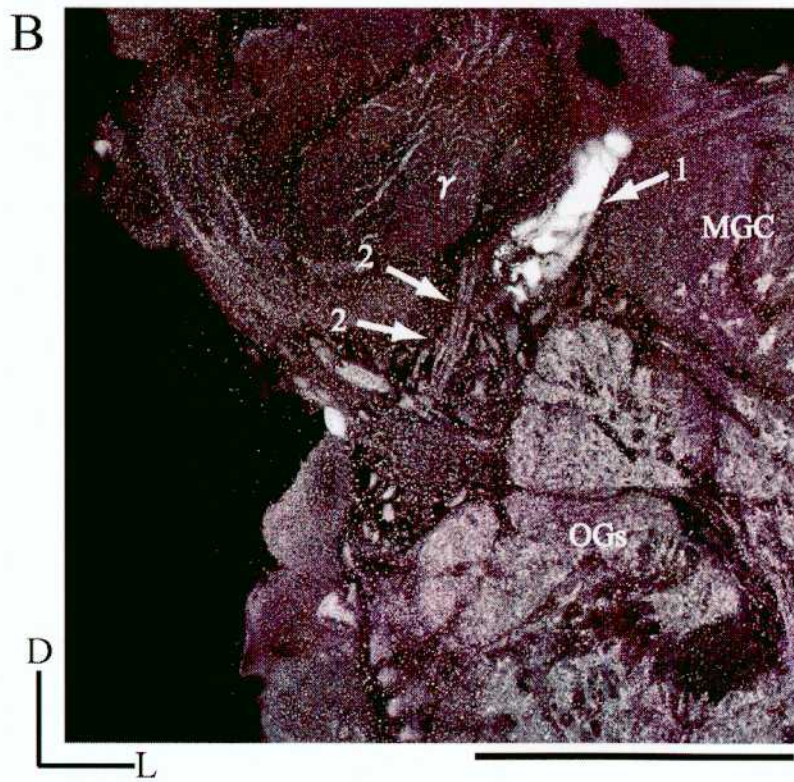
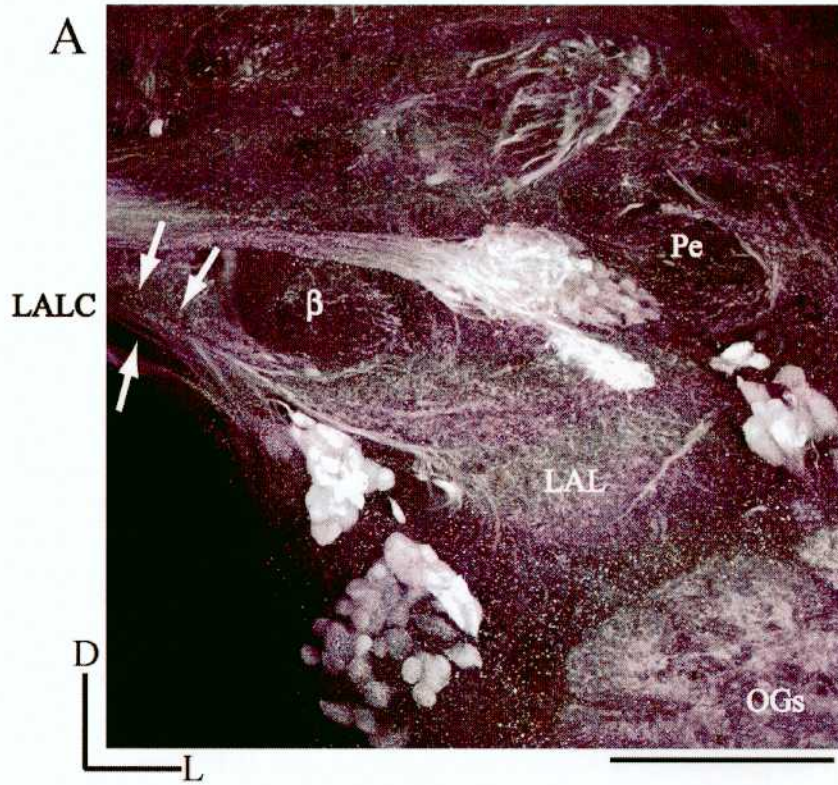


**Fig. 16.** Input region linkage relationship analysis of LAL-BLs. At the morphological input region linkage relationship analysis, I figured the input region tendency in only LAL subregion (vmLAL and dLAL), because none of LAL-BLs had their dendritic arborization only in the VPC. The strong linkage ratio of vmLAL and other subregions was uniform. However in the dLAL, the strong linkage ratio of dLAL and IVPC was remarkably high ratio (63.2%), paralleled with the share ratio of other subregions. Therefore, I regulated ratio for the strong linkage ratio (63.2%), the input subregions tendency were approximately divided into vmLAL main group and dLAL+IVPC pair group.



vmLAL	and	IVPC 46.2%	dLAL 38.5%	mVPC 15.4%	<b>n=10</b>
-------	-----	---------------	---------------	---------------	-------------

dLAL	and	IVPC 63.2%	vmLAL 26.3%	mVPC 10.5%	<b>n=17</b>
------	-----	---------------	----------------	---------------	-------------

**Fig. 17.** Classification of LAL bilateral neuron (LAL-BLs) from their morphological and physiological properties. All the LAL-BLs (represented by deepblue in abbreviation, white in their physiology) received activity from vmLAL, dLAL and IVPC, but not from mVPC, and outputted to the whole area of the contralateral LAL-VPC neural unit. The typical morphological property of TypeA LAL-BLs (represented by green in abbreviation and their physiology) was based on mathematical analysis. They received input from vmLAL and output to vmLAL. Their basic physiological properties defined long-lasting excitation. The typical morphological property of TypeB LAL-BLs (represented by red in abbreviation and their physiology) was based on mathematical analysis. They received input from dLAL and IVPC, and output to vmLAL and dLAL. Their basic physiological property was an inhibitory response. BE: Brief Excitation, BI: Brief Inhibition, Flip-Flop: Flip-Flop activity, LLE: long-lasting excitation, LLI: long-lasting inhibition, NR: not response.

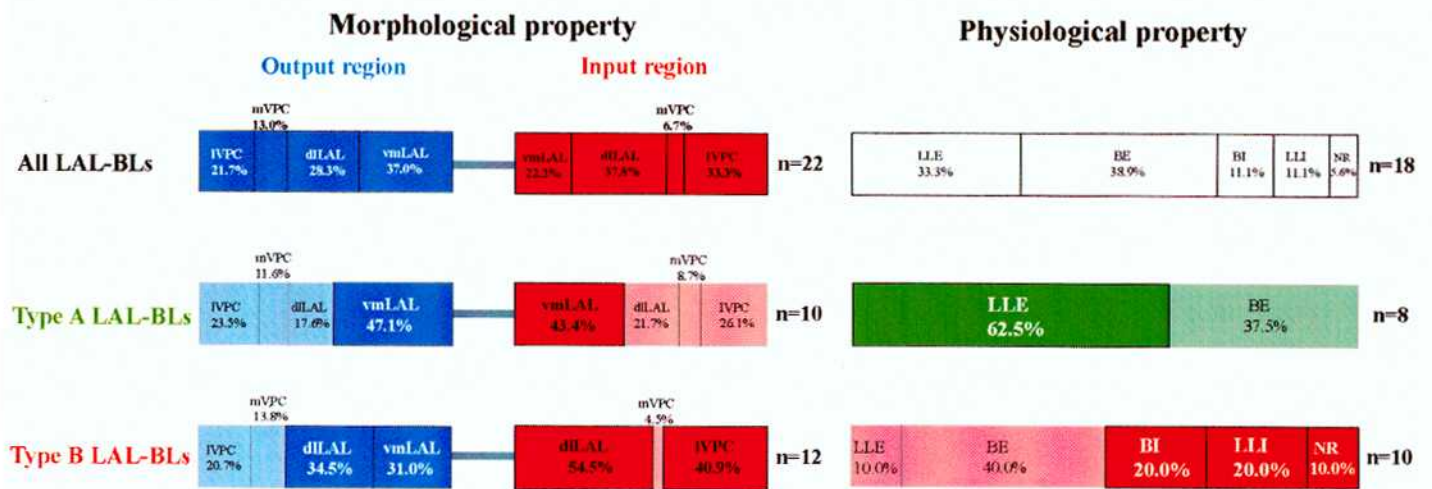


**Fig. 18.** Long-lasting activity generation hypothesis in a side of LAL-VPC neural unit. A) Dorsal superimpose projection image of Type-A LAL-VPC LNs (colored green), Type-B- $\alpha$  LAL-VPC LNs (colored red) and Type-B- $\beta$  LAL-VPC LNs (colored blue). This image was constructed by reference of accurate surrounding neural structures. The coexistence of Type-A LAL-VPC LNs and Type-B- $\alpha$  LAL-VPC LNs output (varicose arborization) could confirm in the LAL-VPC border region (gray thick band), especially thicken in mVPC anterior region (arrow 1). However, Type-B- $\beta$  LAL-VPC LNs, which showed long-lasting activity, had input (dendritic arborization) in mVPC anterior region (arrow 2). B) Frontal projection view of only defined mVPC anterior region. The mVPC anterior region was landmarked by OACT (blue dotted arrow head) and LALC (orange dotted arrow head). Varicose arborizations were observed in Type-A (colored green), and Type-B- $\alpha$  LAL-VPC LNs (colored red). Dendritic arborizations were observed in Type-B- $\beta$  LAL-VPC LNs (colored blue), which showed long-lasting activity. C) Schematic diagram of long-lasting activity generation hypothesis in LAL-VPC neural unit. Type-A (green schematic arrow) and Type-B- $\alpha$  LAL-VPC LNs (red schematic arrow) probably make continuance output to mVPC anterior region. Furthermore Type-B- $\beta$  LAL-VPC LNs (blue schematic arrow) received continuous input from these neurons on the mVPC anterior region and probably output long-lasting activity.

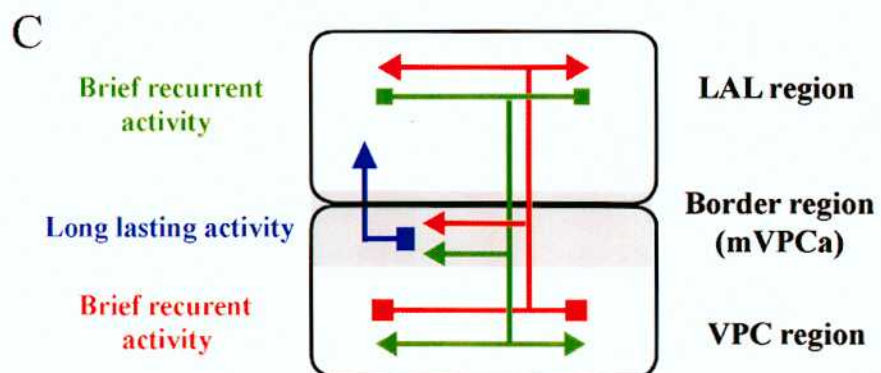
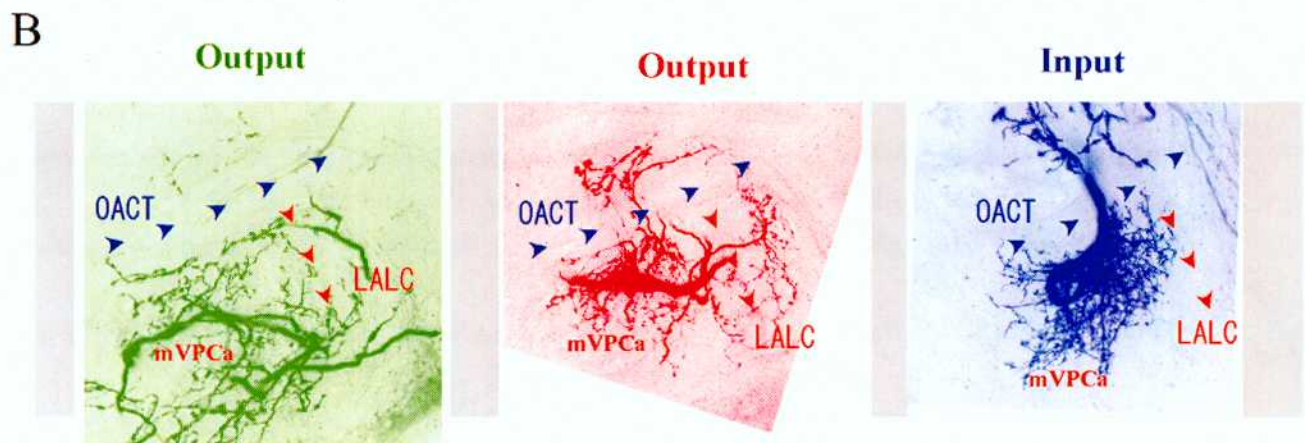
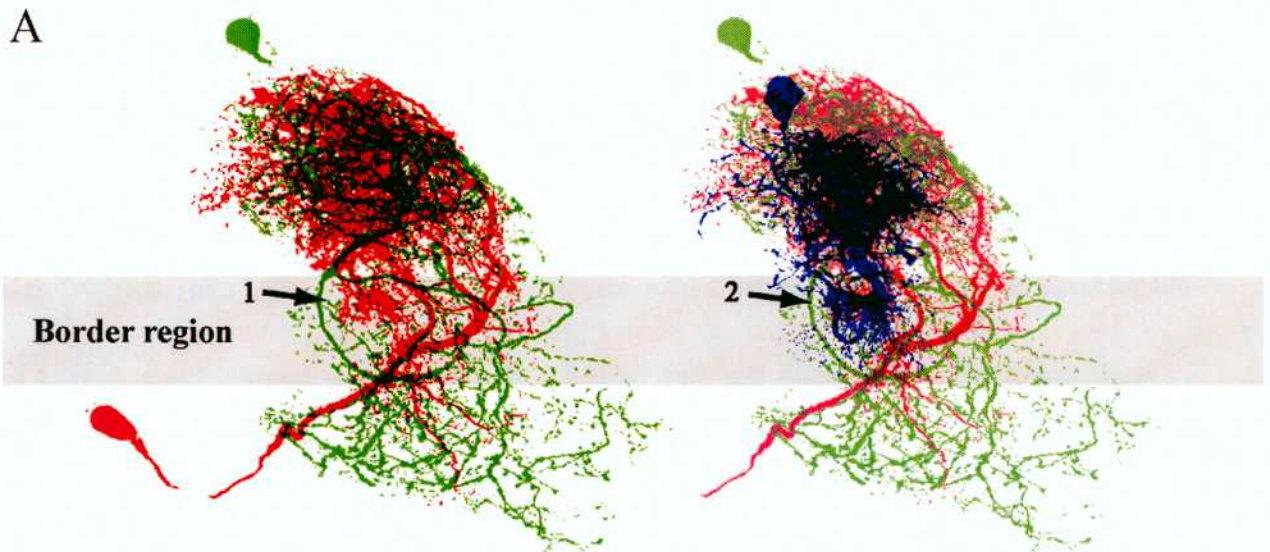


**Fig. 19.** Summary of standard morphological and physiological properties of LAL-VPC intrinsic neurons. A) LAL-VPC LNs transferred activity from the LAL to VPC (green schematic arrow) and from the VPC to LAL (red schematic arrow). They elicited brief excitation or recurrent brief excitation. B) LAL-VPC LNs elicited long-lasting excitation (blue schematic arrow). Numerous of them (3 out of 4) transferred long-lasting activity from mVPC (including mVPCa) to other LAL-VPC region (to the vmLAL, dlLAL and lVPC). Thickness of diagram line showed number of neurons. Thick line showed many neurons observed. C) TypeA LAL-BLs input from vmLAL and output to vmLAL (green schematic arrow). Their basic physiology was a long-lasting excitation. They probably received long-lasting activity from vmLAL. TypeB LAL-BLs input from dlLAL and lVPC, and output to vmLAL and dlLAL (red schematic arrow). Their basic physiology was an inhibitory response including long lasting inhibition. The long-lasting type LAL-VPC LNs (translucent blue schematic arrow) and LAL-DNs (yellow schematic arrow) show additional reference for their relationship.

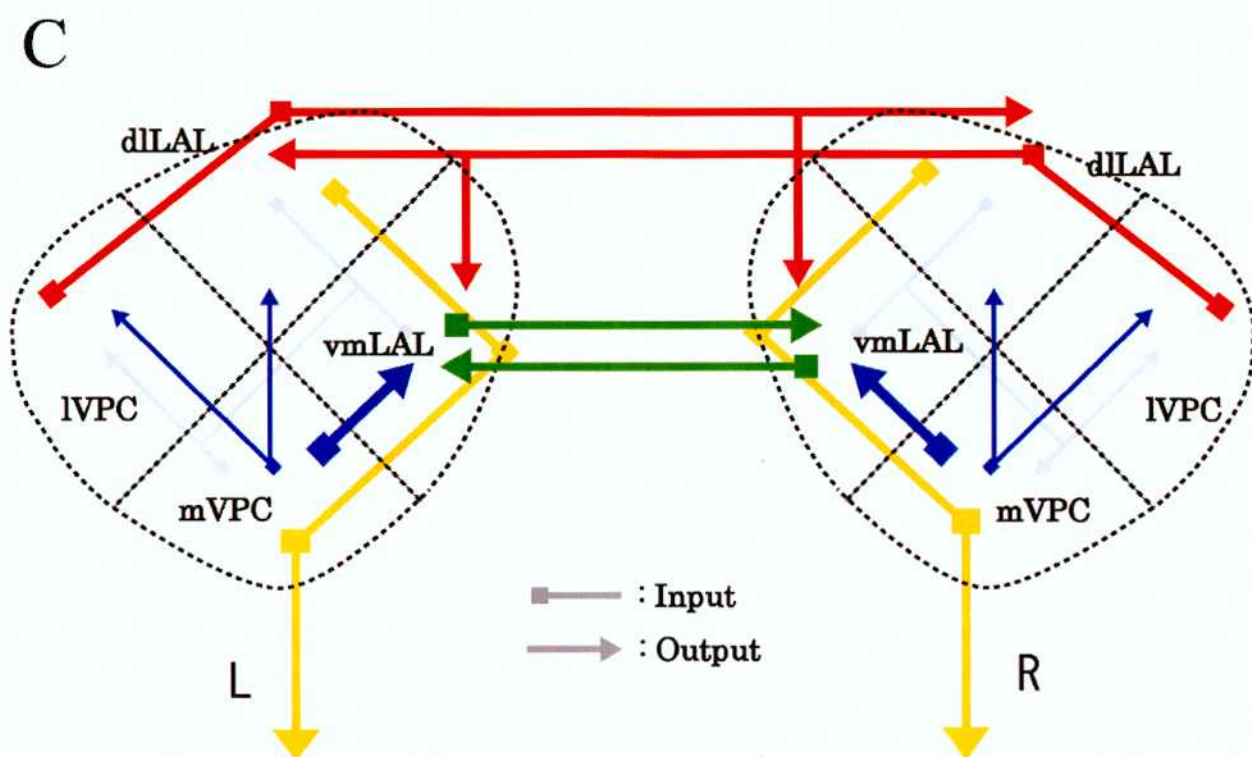
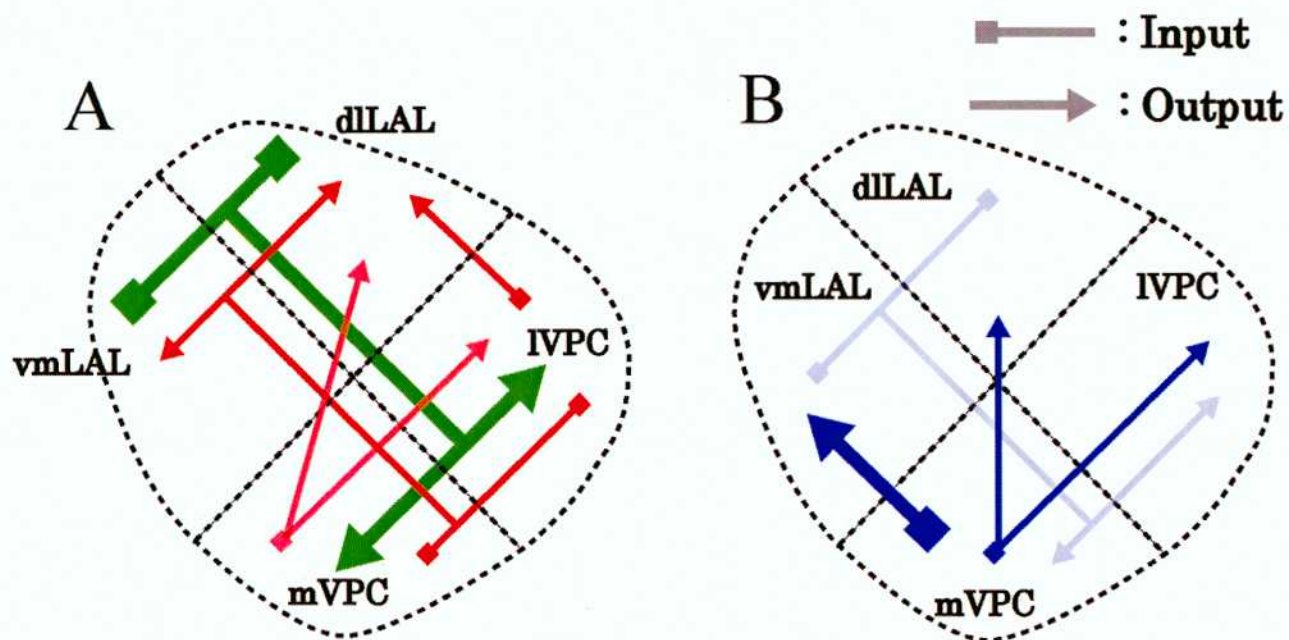
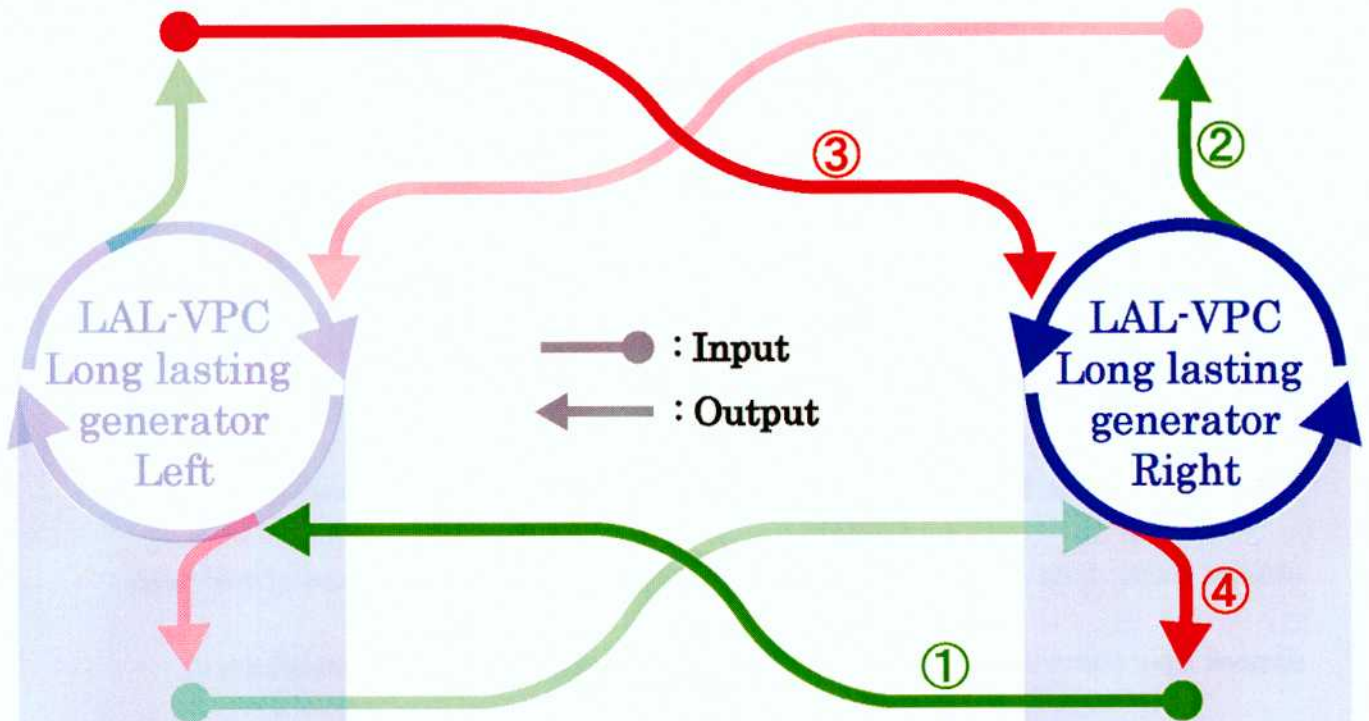


**Fig. 20.** Schematic representation of LAL-VPC neural system, which drives alternating activity pattern in both sides of LAL-VPC neural unit, in the protocerebrum of *B. mori*. Dark color of the arrow show now on activate state, whereas translucent color show now on unactivate state. Blue cyclic arrow show generator of long-lasting activity in a side of LAL-VPC neural unit. Unilateral red arrow ④ show excitatory long-lasting output. Bilateral green arrow ① show Type-A LAL-BLs which receive neural activities from unilateral red arrow ① and elicited long-lasting excitation. Unilateral green arrow ② show inhibitory long-lasting output. Bilateral red arrow ③ show Type-B LAL-BLs which receive neural activities from unilateral green arrow ② and elicited long-lasting inhibition. Type-A LAL-BLs ① may be releasing an inhibitory neurotransmitter to the opposite side through long-lasting excitation activity and perform reciprocal inhibition system. Probably, Type-B LAL-BLs ③ may be releasing an excitatory neurotransmitter to the opposite side through long-lasting inhibition activity and perform reciprocal excitation system in their LAL-VPC neural system. In the schematic representation, I present this pathway by question mark, because their neurotransmitter is not yet identified. Generating alternating activity state in LAL-VPC neural system transfer to the LAL-DNs ⑤ ⑥ as flip-flop activates (FF and ff) and elicit zigzag behavior. LAL-DNs were characterized by Mishima and Kanzaki (1999).



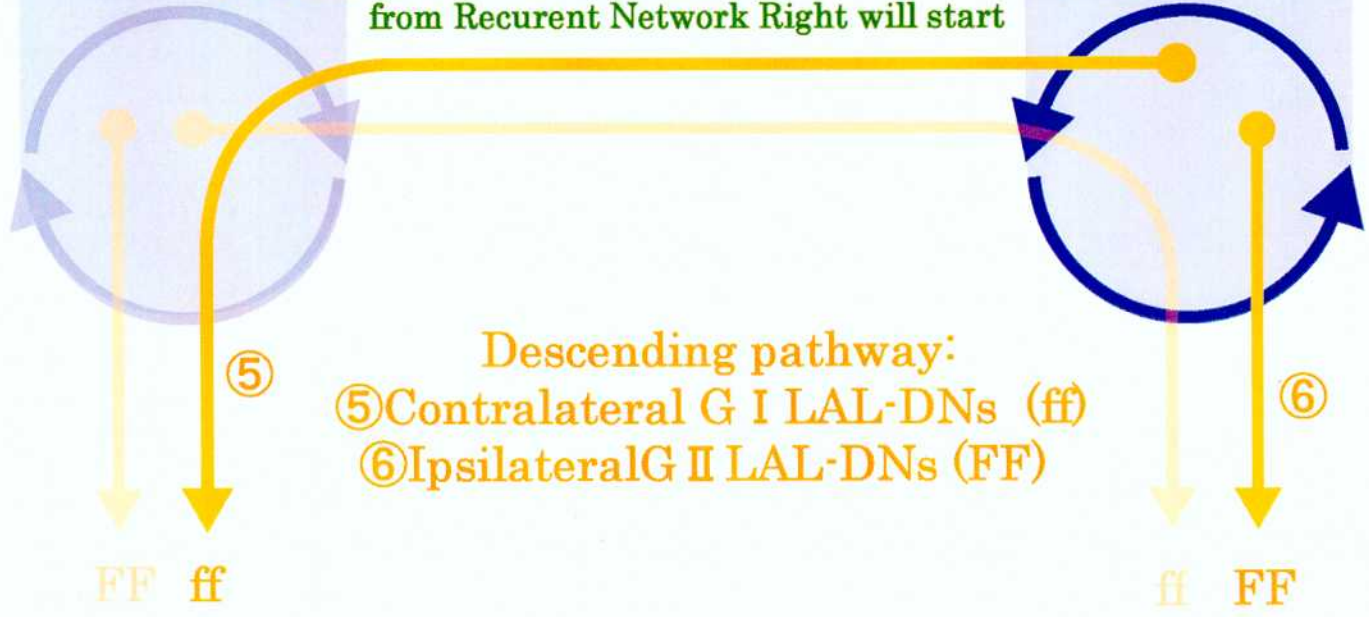
**Excitation pathway?: ③LAL-BLs Type-B(LLI) ④LAL-LNs**

\*Type-B LAL-BLs will be spontaneous burst when Inhibitory activity input from Recurent Network Left will stop



**Inhibition pathway: ①Type-A LAL-BLs (LLE) ②LAL-LNs**

\*Type-A LAL-BLs will be lasting burst when excitatory input from Recurent Network Right will start



**Descending pathway:**

⑤ Contralateral G I LAL-DNs (ff)

⑥ Ipsilateral G II LAL-DNs (FF)







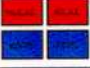














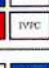


**Fig. 21.** A-C Summary of physiology and morphology of LAL-BLs extracted from the Neuron Database. BE; Brief Excitation, BI; Brief Inhibition, Flip-Flop; Flip-Flop activity, LLE; Long-Lasting Excitation, LLI; Long-Lasting Inhibition, Spontaneous; Spontaneous activity, NON; I do not have physiology data about this neuron. Existence of Red color showed input (dendritic arborization). Blue color showed output (varicose arborization).

# LAL-BLs

Sample code	Physiology type	Morphology				Type
		Output region		Input region		
1	LLE	lLAL IVPC	mLAL mVPC	vLAL mVPC	lLAL lVPC	A
2	LLE	lLAL IVPC	mLAL mVPC	vLAL mVPC	lLAL lVPC	A
3	BI-LLE	lLAL IVPC	mLAL mVPC	vLAL mVPC	lLAL lVPC	A
4	LLE	lLAL IVPC	mLAL mVPC	vLAL mVPC	lLAL lVPC	A
5	BI-LLE	lLAL IVPC	mLAL mVPC	vLAL mVPC	lLAL lVPC	A
6	LLE	lLAL IVPC	mLAL mVPC	vLAL mVPC	lLAL lVPC	B
7	BE	lLAL IVPC	mLAL mVPC	vLAL mVPC	lLAL lVPC	A
8	BE	lLAL IVPC	mLAL mVPC	vLAL mVPC	lLAL lVPC	A
9	BE	lLAL IVPC	mLAL mVPC	vLAL mVPC	lLAL lVPC	A
10	NON	lLAL IVPC	mLAL mVPC	vLAL mVPC	lLAL lVPC	A
11	NON	lLAL IVPC	mLAL mVPC	vLAL mVPC	lLAL lVPC	A
12	BE	lLAL IVPC	mLAL mVPC	vLAL mVPC	lLAL lVPC	B
13	BE	lLAL IVPC	mLAL mVPC	vLAL mVPC	lLAL lVPC	B
14	BE	lLAL IVPC	mLAL mVPC	vLAL mVPC	lLAL lVPC	B
15	BE	lLAL IVPC	mLAL mVPC	vLAL mVPC	lLAL lVPC	B
16	NON	lLAL IVPC	mLAL mVPC	vLAL mVPC	lLAL lVPC	B
17	NON	lLAL IVPC	mLAL mVPC	vLAL mVPC	lLAL lVPC	B
18	BI	lLAL IVPC	mLAL mVPC	vLAL mVPC	lLAL lVPC	B
19	BI	lLAL IVPC	mLAL mVPC	vLAL mVPC	lLAL lVPC	B
20	Spontaneous	lLAL IVPC	mLAL mVPC	vLAL mVPC	lLAL lVPC	B
21	LLI	lLAL IVPC	mLAL mVPC	vLAL mVPC	lLAL lVPC	B
22	LLI	lLAL IVPC	mLAL mVPC	vLAL mVPC	lLAL lVPC	B

**Fig. 22.** A-C Summary of physiology and morphology of LAL-VPC LNs extracted from the Neuron Database. BE; Brief Excitation, BI; Brief Inhibition, Flip-Flop; Flip-Flop activity, LLE; Long-Lasting Excitation, NON; I do not have physiology data about this neuron. Existence of Red color showed input (dendritic arborization). Blue color showed output (varicose arborization).

## LAL-VPC LNs

Sample code	Physiology type	Morphology		Type
		Output region	Input region	
1	BE-BI-BE			A- $\alpha$
2	BE-BI			A- $\alpha$
3	BE			A- $\alpha$
4	BE-BI recurrent			A- $\alpha$
5	NON			A- $\alpha$
6	BE			B- $\alpha$
7	BE			B- $\alpha$
8	BE			B- $\alpha$
9	LLE			A- $\beta$
10	LLE			B- $\beta$
11	Flip-Flop			B- $\beta$
12	LLE			B- $\beta$